EUROPEAN COMMISSION

Community Research

EURATOM

ARCHER

Collaborative Project

Co-funded by the European Commission under the
Euratom Research and Training Programme on Nuclear Energy
within the Seventh Framework Programme

Grant Agreement Number: 269892
Start date: 01/02/2011Duration: 48 Months

www.archer-project.eu

Archer
Advanced Reactor
for Cogeneration of
Heat & Electricity-R&D

Deliverable D-43.11: IHX First Design & Calculation Report

Mohamed S Benguergoura (AL)
F Pra (CEA)

Advanced High-Temperature Reactors for Cogeneration of Heat and Electricity R&D

Document title	Deliverable D-43.11: First Design and Calculation Report
Author(s)	Mohamed S Benguergoura (AL) & F Pra (CEA)
Number of pages	xx
Document type	Deliverable
Work Package	WP43
Document number	D-43-11:
Issued by	D Buckthorpe (AMEC)
Date of completion	31/01./2013
Dissemination level	Confidential, only for consortium members (including the Commission Services)

Summary

A mock-up intermediate heat exchange for future (Very) High Temperature Reactors will be tested within the ARCHER EU Project over the period 2011-2015. This document provides the first design and calculation report on the Design of this Mock-up arrangement. The design calculations involve CFD and FEA using elastic analysis methods carried out within CEA and AL.

Approval

Rev.	Date	First authors	SP leader	Project Coordinator
0	month/year	Franck Pra, CEA Mohamed S Benguergoura, pp. Franck Baurand AL	D Buckthorpe; AMEC	S Groot;NRG
	01/2013			

Distribution list

Name	Organisation	Comments
All beneficiaries	ARCHER	Through internet workspace
WP3 Participants	ARCHER	Through internet workspace

Table of contents

1 Summary

CFD calculations have been performed to provide information on thermal and hydraulic performances that can be reached within the IHX in helium conditions and with mock up in air conditions. The results from such calculations are reported in this document from simulations run with a single plate assuming perfect fluid flow distribution. These data may be used for FEM calculations for the middle plates of a heat exchanger.

In addition it was also necessary to consider the thick end plate and a stack of plates. A full plate geometry has therefore been modelled and the steady state conditions and temperature differences between the plates have been obtained taking into account thermal conditions which are applied outside of the outer plate. Transient conditions have also been applied to this second geometry for He-He IHX and for Air-Air mock-up, showing similar thermal behaviour between both devices,

For assessment of integrity it is necessary to run Finite Element Mechanical (FEM) calculations. The results from the CFD calculations were therefore transferred to the partners in order to carry out this task. One set of results of these calculations based on elastic calculations is given in this report.

The results of the FEM analysis performed by Alfa Laval for the Intermediate Heat Exchanger (IHX) based on the above CFD results have also been attached to this report and consider the following cases:

- Using Alloy 800H material: (the material currently used for IHX module)
  - Under Transient conditions

- Using Inconel 617 material: (this study is given for information because the Inconel 617 material is no longer used for IHX module)
  - Under Steady State conditions
  - Under Transient conditions

All these calculations take into account the thermal inertia of the external plate. The calculations have been carried out using the finite element method in the SYSTUS software version 2010. For this issue first results for steady state and transient analysis of Inconel 617 and Alloy 800H are reported.

2 Contribution from CEA

RESTRICTED DIFFUSION

Rapport technique DST/RT/DR/2013/032

«Project FP7 ARCHER - deliverable D43.11
IHX first design – Calculation report»

Auteur (s) : F.PRA, P.BONNAMY

Référence PRODEM	10-03377
Titre du projet	Projet ARCHER
Type de projet (ANR, CE…)	CE
Période du projet	01/02/2011 – 31/01/2015
Nature du rapport	☐ Rapport d'avancement ☐ Rapport final ☒ Contribution à un rapport global ☐ Rapport de tâche (WP) ☐ Autres : workshop

	Rédacteur	**Vérificateur (s)**	**Approbateur**	**Emetteur**
Nom	PRA F.	P.TOCHON	P.TOCHON	CLAVELIER L.
Fonction	Chargé d'affaires	Chef de laboratoire	Chef de laboratoire	Chef de département
Signature				Accord pour diffusion
Date	11/02/2013	18 /02/2013	18 /02/2013	01/03/2013

Commissariat à l'énergie atomique et aux énergies alternatives
Centre de Grenoble – 17, Avenue des Martyrs
38054 Grenoble Cedex 09

Laboratoire d'innovation pour les technologies
des énergies nouvelles et les nanomatériaux

Département DTS
Laboratoire LETh

Etablissement public à caractère industriel et commercial I RCS Paris B 775 685 019

Imp 113 C

LISTE DE DIFFUSION

Rapport complet signé + Bordereau d'envoi signé à :

AREVA NP	D.LHACEMI	1 ex. (Courriel)
ALFA LAVAL	F.BAURAND	1 ex. (Courriel)
	A.PECHBERTY	1 ex. (Courriel)
	F.RONDET	1 ex. (Courriel)
LITEN	F.LAMBERT	1 ex. (courriel)
DTS	L.CLAVELIER	1 ex. (courriel)
	Ingénieur Qualité DTS (S. SICOT)	1 ex. (courriel)
DTS/LETH	P. TOCHON	1 ex. (courriel)
	F. PRA	1 ex. (courriel)
	Archivage	Original + 1 ex.

Page de garde signée + Liste de diffusion + résumé + Bordereau d'envoi signé à :

Coordinateur Qualité LITEN : J-F. NOWAK
Ingénieur Qualité DTS : S. SICOT
Bureau financier (Ventes) : C.RINCHET, D.STAZIO
Chefs des autres départements du LITEN
Chefs des autres laboratoires du DTS

Confidentialité : Les informations contenues dans le présent document sont la propriété des contractants. Ce document ne peut être reproduit ou transmis à des tiers sans l'autorisation expresse des contractants.

Summary

This document is a contribution of the deliverable D43.11 of WP4.3 of ARCHER European Program.

Within this workpackage, the study is focussed on an Intermediate Heat eXchanger (IHX) for helium nuclear reactor of 4th generation. The studied IHX is a "Plate Stamped Heat Exchanger".

The workpackage 4.3 covers the demonstration of the feasability of an IHX module including :

- the design;
- manufacture of a mock-up made from Alloy 800H;
- tests in the Claire loop at operating conditions (750°C-800°C) to assess the compact IHX, namely PSHE, lifetime.

The document provides the CFD calculations run by CEA for different cases :

- Single plate;
- Stack of plates with external thick plate;
- Either with air (mock-up) or helium (IHX) working conditions;
- Steady and transient conditions.

Temperature fields are extracted from these calculations and transferred to the partners (i.e. NRG & Alfa Laval) to run FEM calculations.

Key words

ARCHER program, IHX, CFD calculation, PSHE, mock-up

Confidentialité : Les informations contenues dans le présent document sont la propriété des contractants. Ce document ne peut être reproduit ou transmis à des tiers sans l'autorisation expresse des contractants.

Imp 113 C

European Commission
Community Research

ARCHER

Collaborative Project

Co-funded by the European Commission under the
Euratom Research and Training Programme on Nuclear Energy
within the Seventh Framework Programme

Grant Agreement Number: 269892

Start date: 01/02/2011 Duration: 48 Months

www.archer-project.eu

Archer
Advanced Reactor
for Cogeneration of
Heat & Electricity-R&D

IHX first design – Calculation report

Franck PRA (CEA)

ARCHER project – Contract Number: 269892
Advanced High-Temperature Reactors for Cogeneration of Heat and Electricity R&D

EC Scientific Officer: Dr. Panagiotis Manolatos

Confidentialité : Les informations contenues dans le présent document sont la propriété des contractants. Ce document ne peut être reproduit ou transmis à des tiers sans l'autorisation expresse des contractants.

Document title	IHX first design – Calculation report
Author(s)	Franck PRA (CEA)
Number of pages	32
Document type	Deliverable
Work Package	WP4
Document number	D43.11 – revision 0
Issued by	CEA
Date of completion	17/12/2012
Dissemination level	Restricted to the partners of the ARCHER project/Public

Summary

This document contains …

Approval

Rev.	Short description	First author	WP Leader	SP leader	Coordinator
0	First issue	PRA (CEA) ../../..	D.LHACEMI (AREVA)	D.BUCKTHORPE	S.de GROOT(NRG) ../../..

Distribution list

Name	Organisation	Comments
P. Manolatos	EC DG RTD	
All technical participants	ARCHER	
Steering Committee members	ARCHER	

Confidentialité : Les informations contenues dans le présent document sont la propriété des contractants. Ce document ne peut être reproduit ou transmis à des tiers sans l'autorisation expresse des contractants.

Imp 113 C

SOMMAIRE

Confidentialité : Les informations contenues dans le présent document sont la propriété des contractants. Ce document ne peut être reproduit ou transmis à des tiers sans l'autorisation expresse des contractants.

Imp 113 C

Introduction

The workpackage 4.3 covers the demonstration of the feasability of an IHX module including :

- the design;
- manufacture of a mock-up made from Alloy 800H;
- tests in the Claire loop at operating conditions (750°C-800°C) to assess the compact IHX, namely PSHE, lifetime.

CFD and FEM calculations are performed on IHX with real working conditions and on mock up with air Claire loop working conditions. CFD calculations aim to predict thermal and hydraulic performances of devices and to provide temperature fields to run FEM calculations. These calculations are run in nominal steady conditions and in transient conditions. CEA runs CFD calculations using FLUENT software and temperature fields are respectivily provided to NRG and Alfa Laval to run FEM calculations for the air mock-up and the real IHX.

I. IHX specifications

IHX is a crucial component for this application and it has to respect different criteria:

- Since it is a barrier between primary and secondary loop, a minimum leak rate is accepted;
- Thermal and hydraulic performances directly impact on the efficiency of the plant, so the higher they are, the better it is;
- It has to resist to extreme mechanical stresses due to nominal working conditions and transient phases: brutal stops, starting procedures;
- Compactness is required to generate a minimum volume and weight to reduce the number of vessels;
- Minimize operation of maintenance;
- Maximise lifespan.

Confidentialité : Les informations contenues dans le présent document sont la propriété des contractants. Ce document ne peut être reproduit ou transmis à des tiers sans l'autorisation expresse des contractants.

Imp 113 C

I.1 IHX working conditions

I.1.1 Steady state

Specifications for the IHX have been provided by AREVA. The nominal working conditions in steady state are given in Table1.

	Primary hot fluid		Secondary cold fluid
Fluid	helium		helium
Mass flow rate (kg/s)	251		251
Inlet Temperature (°C)	750		240
Expected Outlet temperature (°C)	290		700
Expected thermal efficiency (%)		90	
Expected Thermal Duty (MW)		600	
Inlet pressure (bar)	55.1		50.2
Allowed DP (% Pin)	2		2

Table1 : Steady state working conditions for the IHX

I.1.2 Transient working conditions

Different type of transients may occur during reactor life. It was decided to focus the study on one type of thermal transient. The identified transient is supposed to occur once a week corresponding to an occurrence of 1000 for a lifetime of 20 years.

COLD SHOCK: decrease of 200°C (from 750 to 550°C) of the primary fluid at inlet within 5min.
HOT SHOCK: increase of 200°C (from 550 to 750°C) of the primary fluid at inlet within 5min.

Figure 1 shows the temperature profiles at inlet of primary and secondary fluids during such a transient.

Confidentialité : Les informations contenues dans le présent document sont la propriété des contractants. Ce document ne peut être reproduit ou transmis à des tiers sans l'autorisation expresse des contractants.

Imp 113 C

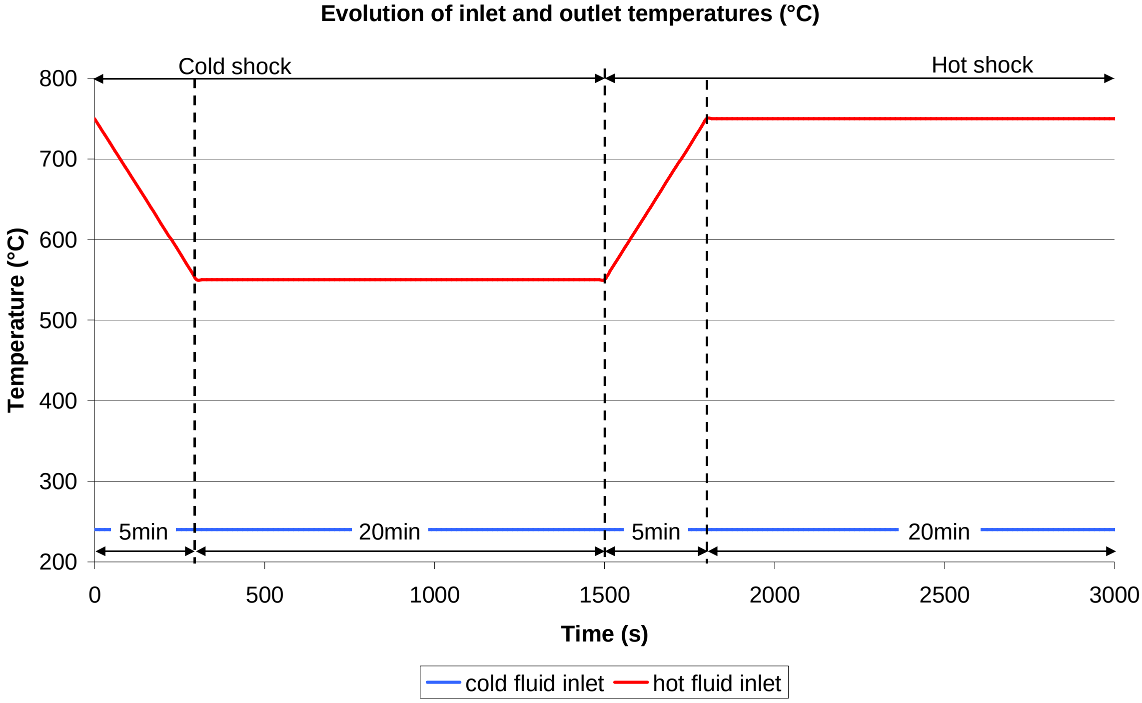

Figure 1 : Temperature profiles during transient

I.2 Air mock-up working conditions

Within the project, the technical feasibility of such an IHX has to be proven. Consequently, a mock-up is manufactured. This gives the opportunity to test it on a test rig. Choices have to be made to size this mock up taking into account the following points:

- The available test loop is an open air loop with mass flow rates of 0.18 kg/s;
- The whole IHX is made of 128 modules, each module being a stack of 165 plates.

So it was decided to manufacture a mock-up respecting the length and the width of the real IHX and to adapt the number of plates so that the Reynolds numbers are respected between helium IHX and air mock up.

From thermal and hydraulic point of views, IHX and mock-up should have the same behaviour. Considering thermo mechanical aspects, it is clear that the behaviour will be different. From past experience, it was admitted it would be necessary to keep the length and the height of the stack to generate the same creep damages. To accelerate the creep damages on mock up, it was decided to increase the temperatures on both sides of 50°C.

Confidentialité : Les informations contenues dans le présent document sont la propriété des contractants. Ce document ne peut être reproduit ou transmis à des tiers sans l'autorisation expresse des contractants.

I.2.1 Steady state

The nominal working conditions in steady state on the mock up are given in Table 2.

	Primary hot fluid		Secondary cold fluid
Fluid	Air		Air
Mass flow rate (kg/s)	0.18		0.18
Inlet Temperature (°C)	800		290
Expected Outlet temperature (°C)	340		750
Expected thermal efficiency (%)		91	
Expected Thermal Duty (kW)		91.5	
Inlet pressure (bar)	6.3		3.8
Max allowed DP (bar)	6.3		3.8

Table 2: Steady state working conditions for the mock-up

I.2.2 Transient working conditions

Same transients of temperature than IHX ones will be applied be to the mock up starting from initial temperatures 50°C higher.

II. IHX and mock-up dimensions

CEA, AREVA and ALFA LAVAL have been working for several years on a compact IHX concept made of corrugated plates, namely PSHE (Stamped Plate Heat Exchanger). The research and development carried out these last years gave encouraging results and lead to improvement of reliability, mechanical strength and lifespan of the concept. First analytical and numerical calculations allowed fixing the geometry of the IHX.

II.1 Plate specifications and dimensions

The active area of the plate is made of corrugated plates. The corrugations are generated by stamping of Incoloy plates. The plate thickness is 1.5 mm and the depth of corrugation is 1.5 mm as well.

Confidentialité : Les informations contenues dans le présent document sont la propriété des contractants. Ce document ne peut être reproduit ou transmis à des tiers sans l'autorisation expresse des contractants.

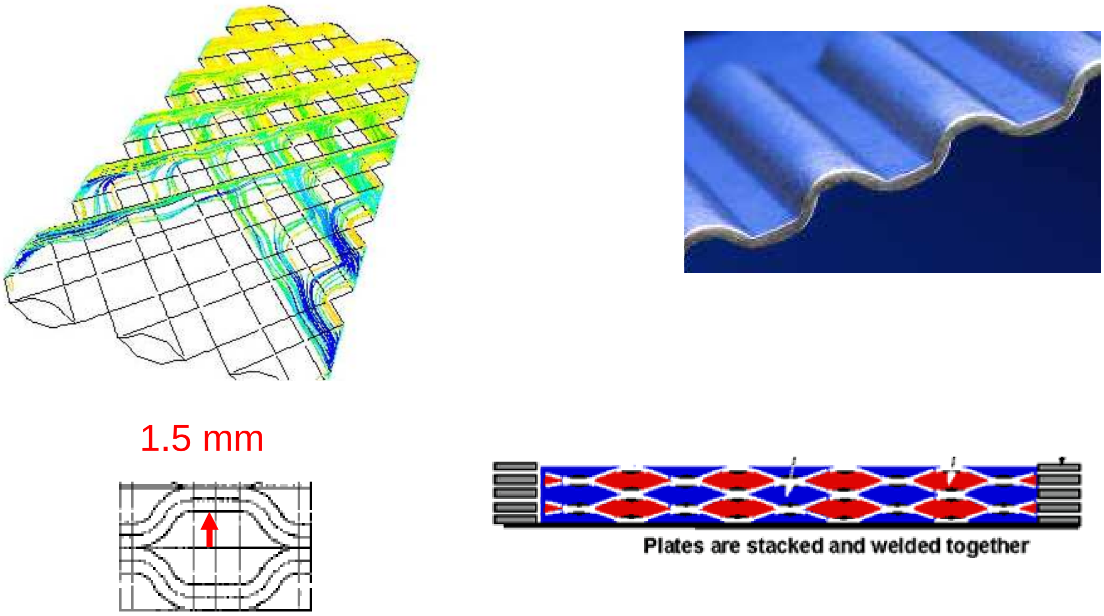

Figure 2 : Illustration of the corrugation and flow pattern generated by CFD simulation in such geometry

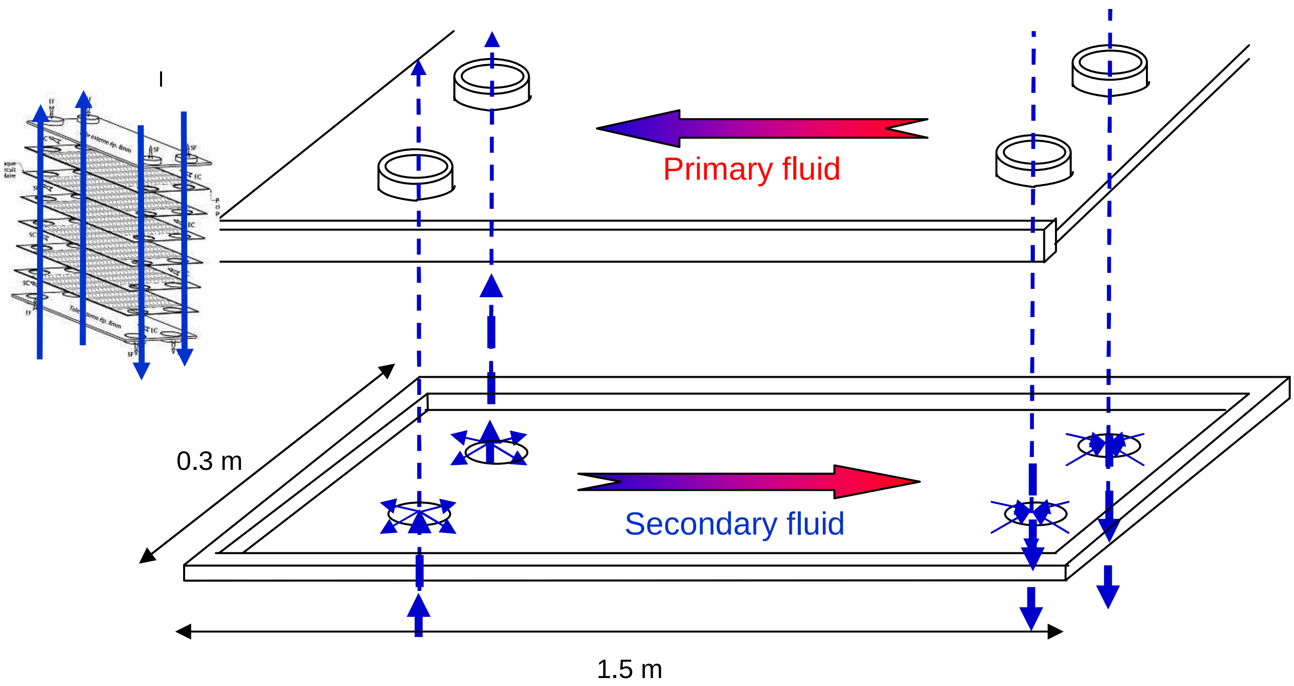

Figure 3 : Illustration of flow circulation within the plates

Confidentialité : Les informations contenues dans le présent document sont la propriété des contractants. Ce document ne peut être reproduit ou transmis à des tiers sans l'autorisation expresse des contractants.

Imp 113 C

II.2 Global dimensions

Tables 3 and 4 provide the main dimensions of the whole He-He IHX and those of the air – air mock-up.

HE-HE IHX	
Length (m)	1.5
Active width (m)	0.294
Height of one module (m)	0.495
Number of modules	128
Number of plates /module	165
Total ZA volume (m^3)	20.9
Total volume (m^3)	28.5

Table 3: Geometrical data of the IHX

AIR-AIR MOCK-UP	
Length (m)	1,5
Active length (m)	0,294
Height of one module (m)	0,048
Number of modules	1
Number of plates /module	16
Total ZA volume (m^3)	0,016
Total volume (m^3)	0,022

Table 4: Geometrical data of the mock-up

III. Numerical simulations

2 types of geometry were modeled:

- Single plate with half fluid channels on both sides of the plate: using specific thermal and hydraulic laws dedicated to such corrugations allows checking thermal performances and pressure drops assuming perfect fluid distribution on both sides.

- Multiple plates: modeling 4 last plates with thick external plate gives further information about fluid distribution and temperature fields dedicated to FEM analysis.

III.1 Modelled geometries

Confidentialité : Les informations contenues dans le présent document sont la propriété des contractants. Ce document ne peut être reproduit ou transmis à des tiers sans l'autorisation expresse des contractants.

Imp 113 C

The « Single plate geometry » is composed of one corrugated plate and two half channels (figure 4). Symmetric plans are used to reduce the size and the number of meshes of the model.

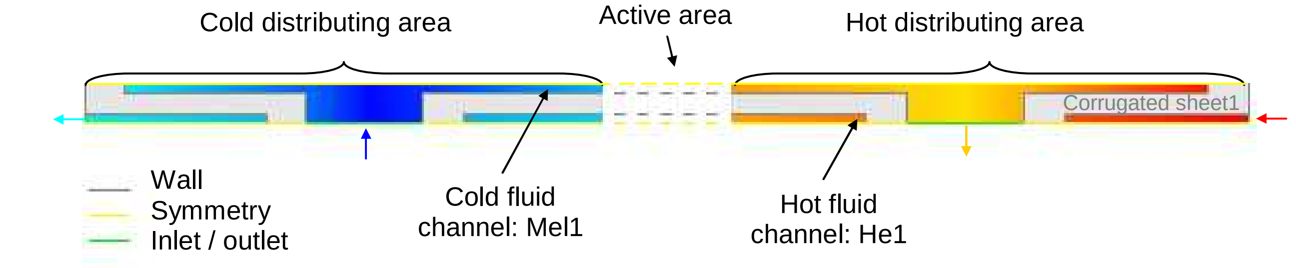

Figure 4 : Single plate geometry

The « Full plate geometry » is composed of the bottom end plate and four corrugated plates. We also have three hot channels (He) and two cold ones (Mel) (figure 5). Of course, calculations are longer with this geometry but thermal inertial effects are taken into account during transient time.

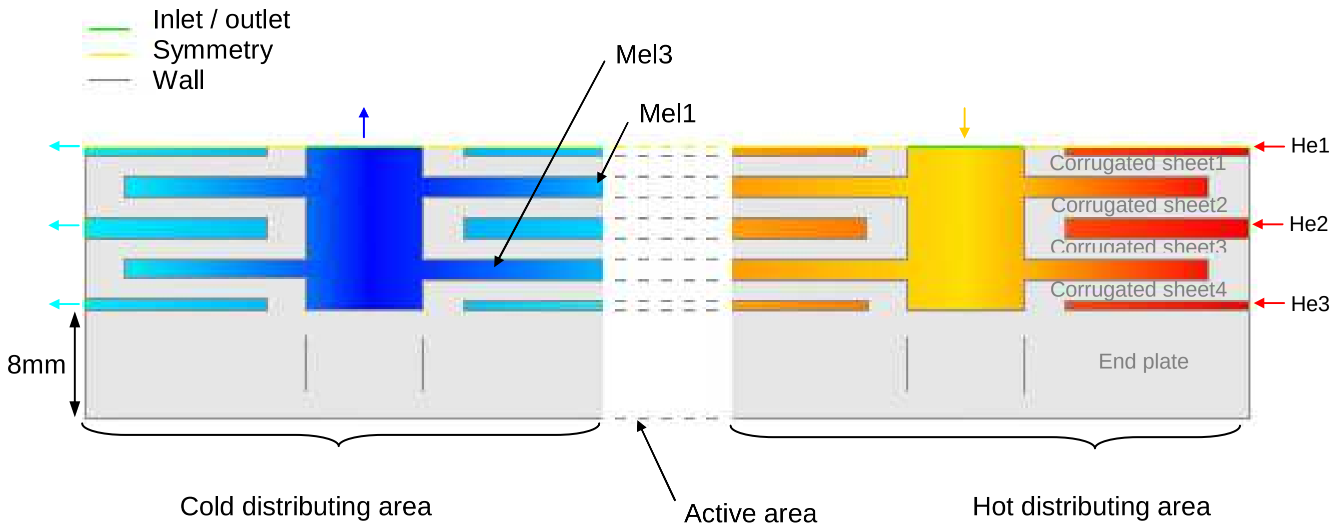

Figure 5 : Multiple plates geometry with external plate

- He1 is an entire channel cut in two parts with a symmetric condition.
- He3 has been set as an half channel of 0.75mm height (whole channels are 1.5mm height)

The geometry of he-he IHX and air-air mock-up has been modified several times. Thus the height of the channel He3 has been affected. So, to adjust the numerical "full plate geometry" to new dimensional specifications, a porosity model was included and the porosity factor was adapted.

Confidentialité : Les informations contenues dans le présent document sont la propriété des contractants. Ce document ne peut être reproduit ou transmis à des tiers sans l'autorisation expresse des contractants.

Indeed we simulated a reduction or an increase of the cross section area in the selected zone without remodelling the whole geometry.

Figure 6 shows a top view of a half plate on hot and cold sides.

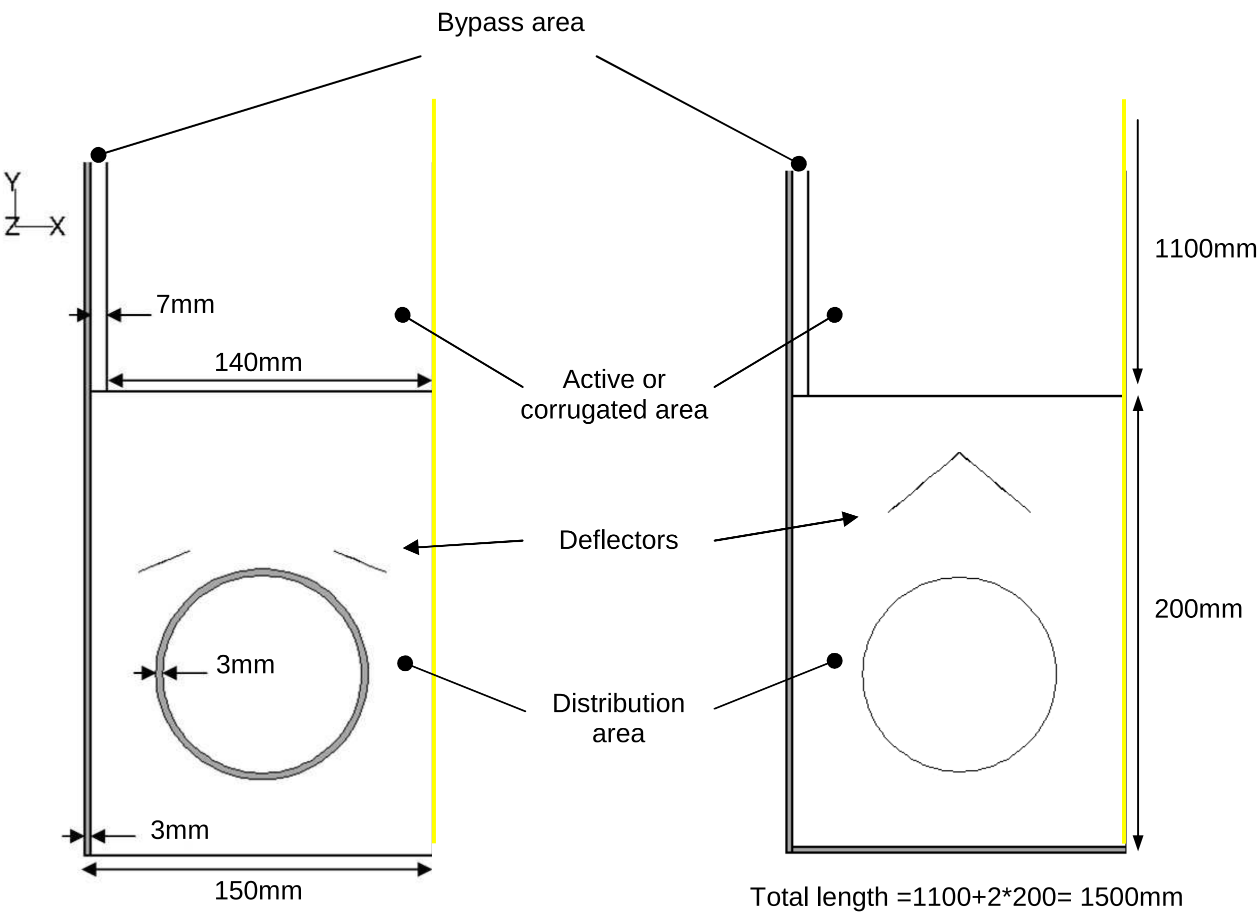

Figure 6 : Corrugated plate on primary and secondary fluid sides

As said previously, symmetric planes (in yellow) are used to reduce the number of meshes. Each plate is divided into 4 zones:

- 2 distributing areas (on hot side and cold side)
- The active area
- The bypass area

Deflectors are set on both sides (cold and hot) as “wall” but they can easily be removed by setting them into “interior”.

Confidentialité : Les informations contenues dans le présent document sont la propriété des contractants. Ce document ne peut être reproduit ou transmis à des tiers sans l'autorisation expresse des contractants.

Imp 113 C

Thermal and hydraulic laws are manually set.

- In distributing areas, conventional laws are used: Blasius, Gnielinski laws whereas specific laws are used in corrugated areas (active area of the plates).
- A porous model is applied to simulate a reduction or an increase of the cross section area in channels (in distributing areas, inserts are used and they induce a modification of the free flow section).

In distributing areas Blasius & Gnielinski laws are applied. Flow within inserts is quite well described by this approach. Hydraulic diameter and porosity factor are fitted to the size of channels:

- *Porosity factor = real cross section area / cross section area in the numeric geometry*
- *Hydraulic diameter = channel's real height*

Remark: Distributing areas are considered as homogeneous and opened. Pins or corrugations which could modify flow lines in distributing zones aren't modelled.

In entire channels of active areas where specific thermal and hydraulic laws for corrugated plates are used, hydraulic diameter is set as 2.597mm.

In half channels of active areas we consider a flow throw tubes with the following characteristics:

- Hydraulic diameter : 1.5mm (stamping height)
- Developed length is equal to the straight length multiplied by 1/cos(30°) due to the angle of corrugation.

Blasius &Gnielinski correlations are used.

In our simulations we considered bypass zones as active zones since the width was not clearly known at this time of calculation.

<u>Hypothesis used for CFD calculations:</u>

All simulations have been done with the following boundary conditions:

- Air-air mock-up is insulated from the external environment

<u>Confidentialité</u> : Les informations contenues dans le présent document sont la propriété des contractants. Ce document ne peut être reproduit ou transmis à des tiers sans l'autorisation expresse des contractants.

Imp 113 C

- He IHX is immerged into the primary fluid: the hot side into the inlet fluid and cold side is into the outlet fluid; the convection factor is set as 5W/m²/°C
- Mass flow rates are set as 11.25g/s per entire channel (5.625g/s for half channels)
- Bypass areas are considered as active parts so that the total active width is 294mm.
- Deflectors are set in both hot and cold zones
- A porosity factor of 0.666 is applied in distributing zones

Thermal and hydraulic laws :

	Distributing zones	**Active and by-pass zones**
Half channels (h=0.75mm)	Blasius & Gnielinski $Dh = 0.5mm$ $poro = 0.666$	Blasius & Gnielinski $Dh = 1.5mm$ $R_1 = 1/\cos(30°)$
Entire channels (h=1.5mm)	Blasius & Gnielinski $Dh = 1mm$ $poro = 0.666$	Specific laws for corrugated plates $Dh = 2.597mm$

III.2 Steady state simulations

III.2.1 « Single plate geometry », air-air mock-up and he-he IHX

Main results obtained with helium and with air are given in Table 5.

Confidentialité : Les informations contenues dans le présent document sont la propriété des contractants. Ce document ne peut être reproduit ou transmis à des tiers sans l'autorisation expresse des contractants.

Imp 113 C

		Primary hot fluid	Secondary cold fluid	Primary hot fluid	Secondary cold fluid
	Fluid	**He**	**He**	**Air**	**Air**
	INLET DATA				
	Total mass flow rate (kg/s)	251	251	0,18	0,18
	Inlet temperature (°C)	750	240	800	290
	Outlet pressure (bar)	54	49,4	5	2,5
Using	Expected outlet temperature (°C)	290	700	340	750
specifications	Expected thermal efficiency (%)	90		91	
	Expected thermal duty (kW)	600		91,5	
	SIZING				
	Number of modules	128		1	
	Number of plates / module	166		16	
	Number of channels	83	82+2*1/2	8	7+2*1/2
	EXCEL results : based only on ZA				
	Reynolds	3726	3895	3458	3568
	DP Active Area (% Pin)	1,1	1,2	12	32
	Predicted outlet temperature (°C)	281	709	331	763
	Predicted efficiency (%)	91,8		92,7	
	Predicted thermal duty (kW)	$610.\ 10^3$		93,7	
Results					
	FLUENT results with distributing area contribution				
	DP Active Area (% Pin)	1,1	1,2	11	27
	DP Total (% Pin)	2,1	1,6	20	35
	Predicted outlet temperature (°C)	**284**	**708**	**335**	**762**
	Predicted efficiency (%)	91,5		91,2	
	Predicted thermal duty (kW)	$607.\ 10^3$		92,2	

Table 5: Main results of both geometries in steady state for a single plate

Remarks:

We have to be careful concerning total pressure losses through the IHX:

- Simulations have been carried out with deflectors at both sides of the IHX. If deflectors are removed at cold side, pressure losses will seriously decrease.
- Pressure losses in distributing areas are modelled with an homogeneous and opened area and we don't take into account pins or corrugations that can impact flow lines.

Expected thermal and hydraulic performances are quite fulfilled:

Confidentialité : Les informations contenues dans le présent document sont la propriété des contractants. Ce document ne peut être reproduit ou transmis à des tiers sans l'autorisation expresse des contractants.

Imp 113 C

- Max pressure losses in he-he IHX are 2.1% of inlet pressure against 2% expected.
- Thermal efficiency of the he-he IHX is 91.5% against 90% required

Figure 7 shows temperature distribution of the plate in hot part of the plate. The collector is a critical area from thermo-mechanical point of view. Deflectors were positioned aiming a decrease of thermal gradient around the collector.

Remark concerning the level of temperature in figure 7: in air-air configuration, inlet temperature is 50°C higher and consequently the level of temperature is higher on the right below picture.

He-He IHX

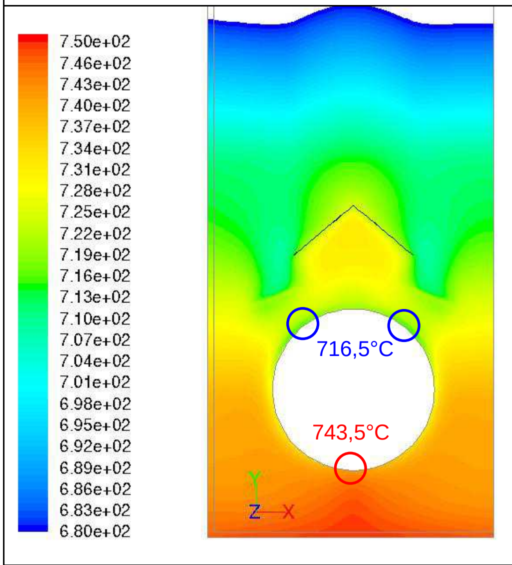

DT around outlet tube = 27°C

Air-Air mock -up

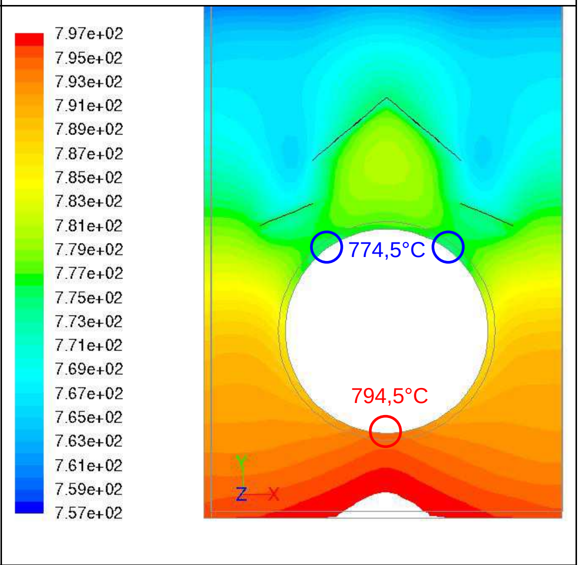

DT around outlet tube = 20°C

Figure 7 : Visualisation of temperature fields around collector in hot part of the plate

Temperature difference around collector of the air-air mock-up is about 7°C lower than those in the he-he IHX. However temperature of air-air mock-up is 50°C higher. So we may consider those phenomenons are balancing themselves.

FEM calculations should check if air-air mock-up and he-he IHX will have the same mechanical behaviour.

III.2.2 « Full plate geometry », he-he IHX

Main results obtained with helium in full plate geometry are given in Table 6.

Confidentialité : Les informations contenues dans le présent document sont la propriété des contractants. Ce document ne peut être reproduit ou transmis à des tiers sans l'autorisation expresse des contractants.

	Primary hot fluid			Secondary cold fluid	
Channels' name	**He1**	**He2**	**He3**	**Mel1**	**Mel3**
INLET DATA					
Mass flow rate (g/s)	5,625	11,25	5,625	11,25	11,25
Inlet Temperature (°C)	750	750	750	240	240
Outlet pressure (bar)	54	54	54	49,4	49,4
Expected Outlet temperature (°C)	290	290	290	700	700
Expected Thermal Duty (W)	13432	26863	13432	-26863	-26863
FLUENT results with distributing area contribution					
za (%Pin)	1,1	1,1	0,6	1,2	1,2
tot (%Pin)	2,1	2,0	2,0	1,6	1,6
Predicted outlet temperature (°C)	284	284	**293**	708	**701**
Predicted thermal Duty (W)	14380	28684	14076	-28955	-29790

Table 6: Main results in steady state for a full plate geometry in helium

Thermal inertial effects of end plates are visible looking at the outlet temperature differences between entire channels in the centre of IHX and half channels:

- Outlet temperature of He3 channel is 293°C and 284°C for He1 and He2.
- Outlet temperature of Mel3 channel is 701°C against 708°C for Mel1.

Also there are some boundary effects that impact temperature profiles and thermo-mechanical strain: they are issued from half channels, top and bottom end plates, and from external conditions.

« Single plate geometry » is satisfying to predict thermal and hydraulic performances, but **« Full plate geometry » is necessary to calculate thermo-mechanical strain into the IHX.**

Temperature profiles of the different plates at the hot side of the IHX are shown in figure 8.

Confidentialité : Les informations contenues dans le présent document sont la propriété des contractants. Ce document ne peut être reproduit ou transmis à des tiers sans l'autorisation expresse des contractants.

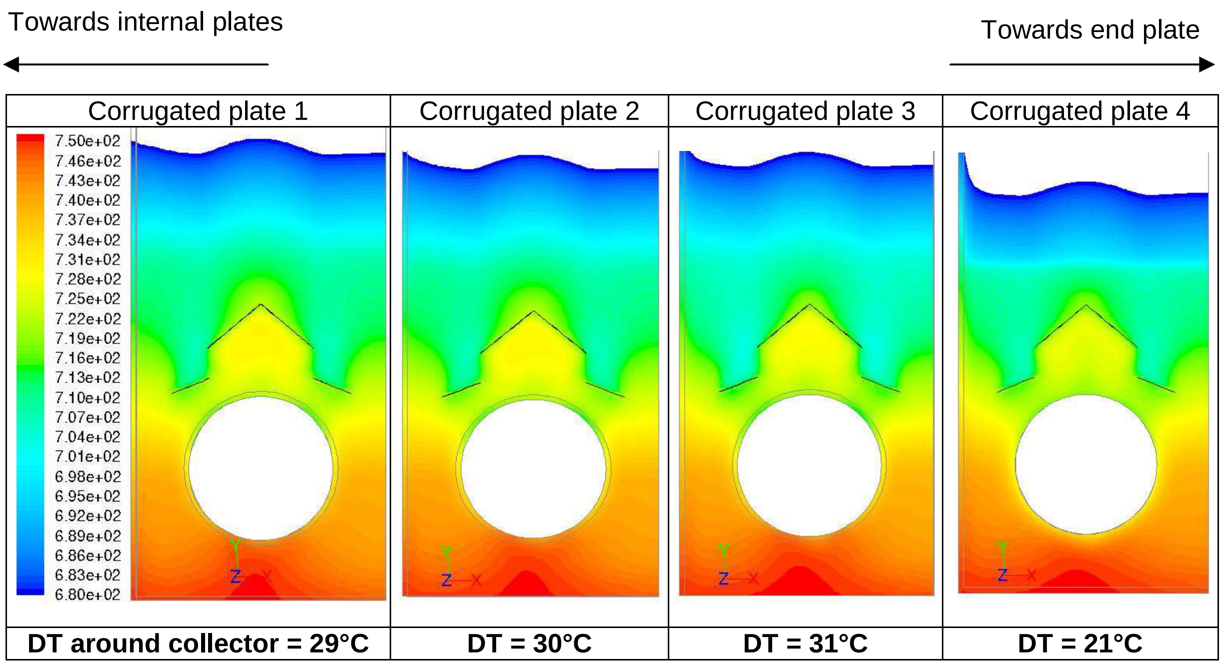

<u>Figure 8 :</u> Visualisation of temperature fields around collector in hot part of the IHX

We can also see on these pictures the thermal inertial effects of end plates:

- On corrugated plate4 which is welded to the bottom end plate, DT is 21°C
- DT around collector of plate3 is the highest one with 31°C
- DT around collector of other interior plates tends to 27°C (equal to value obtained with the “single plate geometry”)

Next figure presents the temperature profile of the bottom end plate (middle plan of the plate).

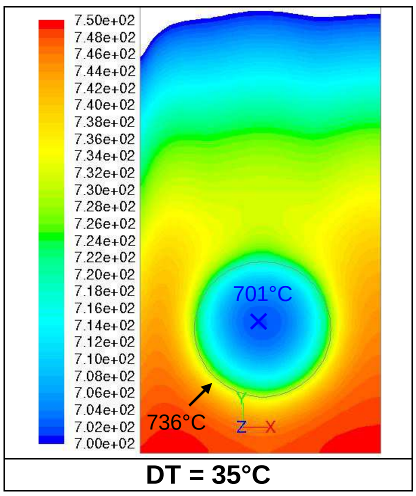

<u>Figure 9 :</u> Bottom end plate temperature

<u>Confidentialité</u> : Les informations contenues dans le présent document sont la propriété des contractants. Ce document ne peut être reproduit ou transmis à des tiers sans l'autorisation expresse des contractants.

Imp 113 C

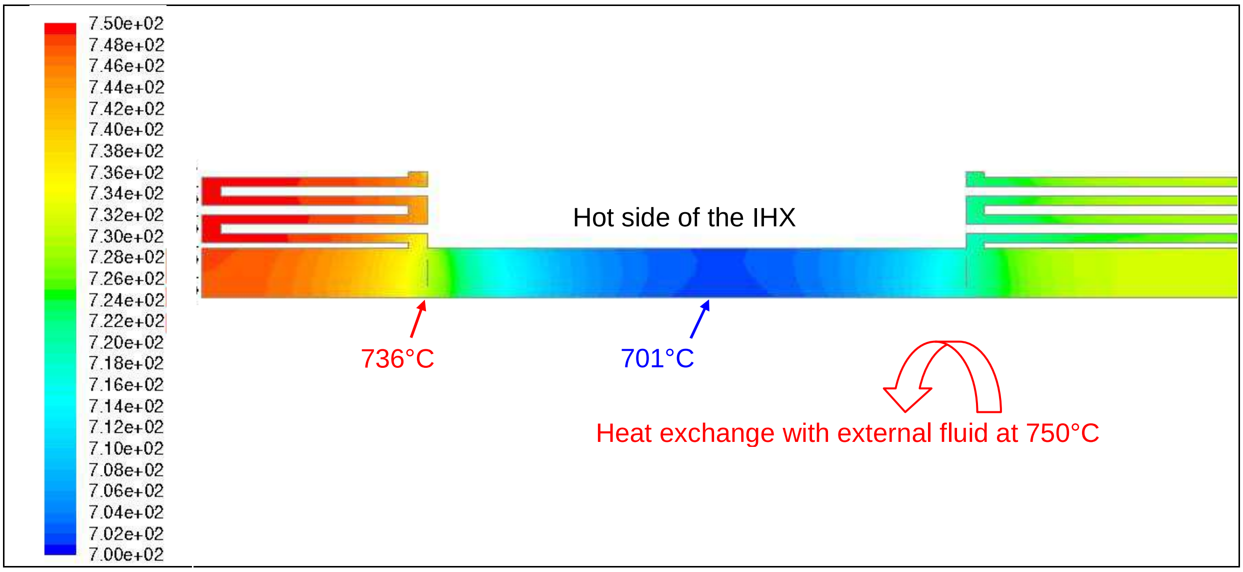

Figure 10 : Temperature longitudinal field near the collector of the hot part of the IHX

Figure 9 and 10 show that the highest temperature difference in this area is reached in the bottom end plate and not in the plate with fluid.

III.2.3 « Full plate geometry », air-air prototype

Main results obtained with air in full plate geometry are given in Table 7.

	Primary hot fluid			Secondary cold fluid	
Channels' name	**Air1**	**Air2**	**Air3**	**Mel1**	**Mel3**
INLET DATA					
Mass flow rate (g/s)	5,625	11,25	5,625	11,25	11,25
Inlet Temperature (°C)	800	800	800	290	290
Outlet pressure (bar)	5	5	5	2,5	2,5
Expected Outlet temperature (°C)	340	340	340	750	750
Expected Thermal Duty (W)	2852	5704	2852	-5704	-5704
FLUENT results with distributing area contribution					
DP active area (%Pin)	11	11	5,7	27	27
DP total (%Pin)	20	20	20	35	35
Predicted outlet temperature (°C)	333	335	**341**	761	**758**
Predicted thermal Duty (W)	2893	5768	2873	-5835	-5790

Table 7: Main results in steady state for a full plate geometry in air

Confidentialité : Les informations contenues dans le présent document sont la propriété des contractants. Ce document ne peut être reproduit ou transmis à des tiers sans l'autorisation expresse des contractants.

Imp 113 C

As in helium, the outlet temperature is different from one plate to another. Thermal inertia of bottom end plate impacts temperatures inside the mock-up:

- Air3 outlet temperature is higher than Air1 and Air2 outlet one;
- Mel3 outlet temperature is lower than Mel1 outlet one.

Temperature profiles of the different plates at the hot side of the mock-up are shown in figure 11.

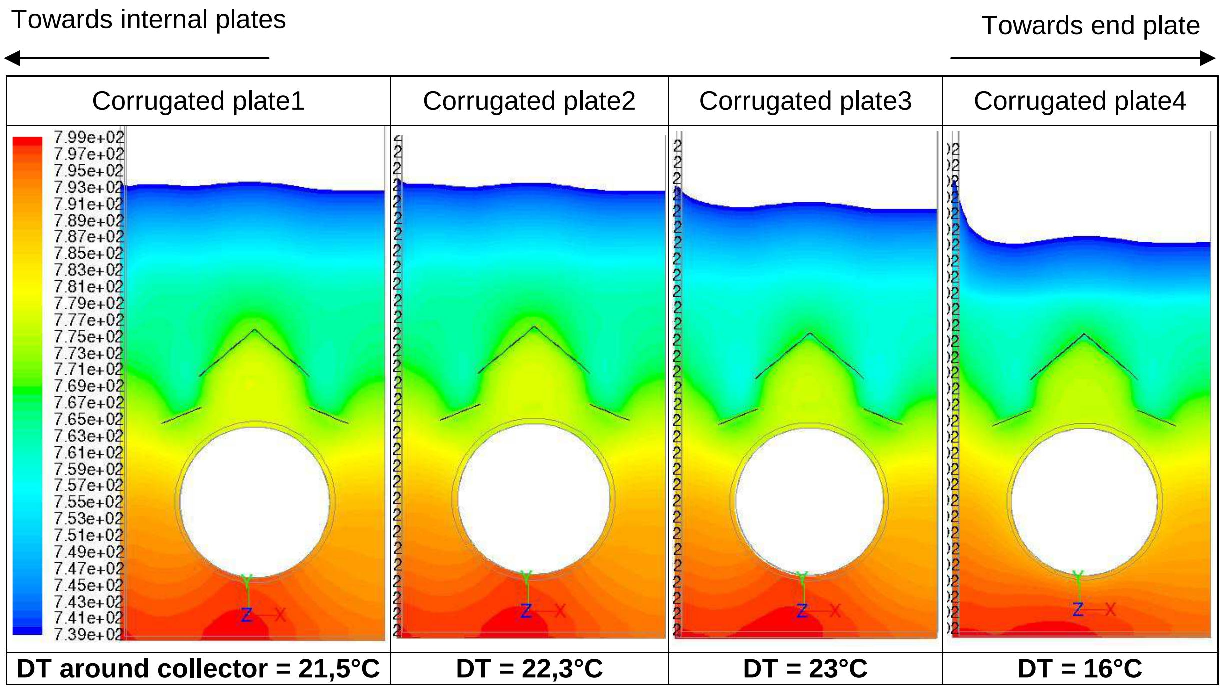

Figure 11 : Visualisation of temperature fields around collector in hot part of the mock-up

We can also see on these pictures the thermal inertial effect of end plates:

- On corrugated plate4 which is welded to the bottom end plate, DT is 16°C
- DT around collector of plate3 is the highest with 23°C
- DT around collector of other inner plates tends to 20°C (equals to value obtained with the "single plate geometry").

Next figure presents the temperature profile of the bottom end plate (middle plan of the plate).

Confidentialité : Les informations contenues dans le présent document sont la propriété des contractants. Ce document ne peut être reproduit ou transmis à des tiers sans l'autorisation expresse des contractants.

Imp 113 C

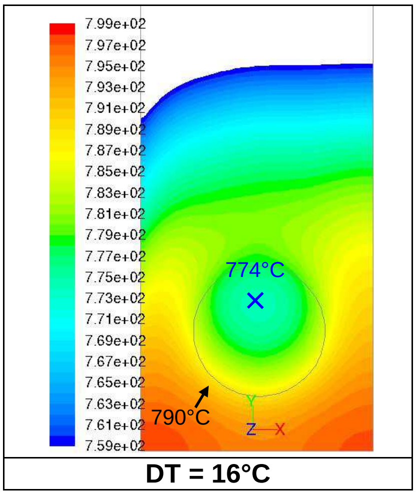

Figure 12 : Bottom end plate temperature

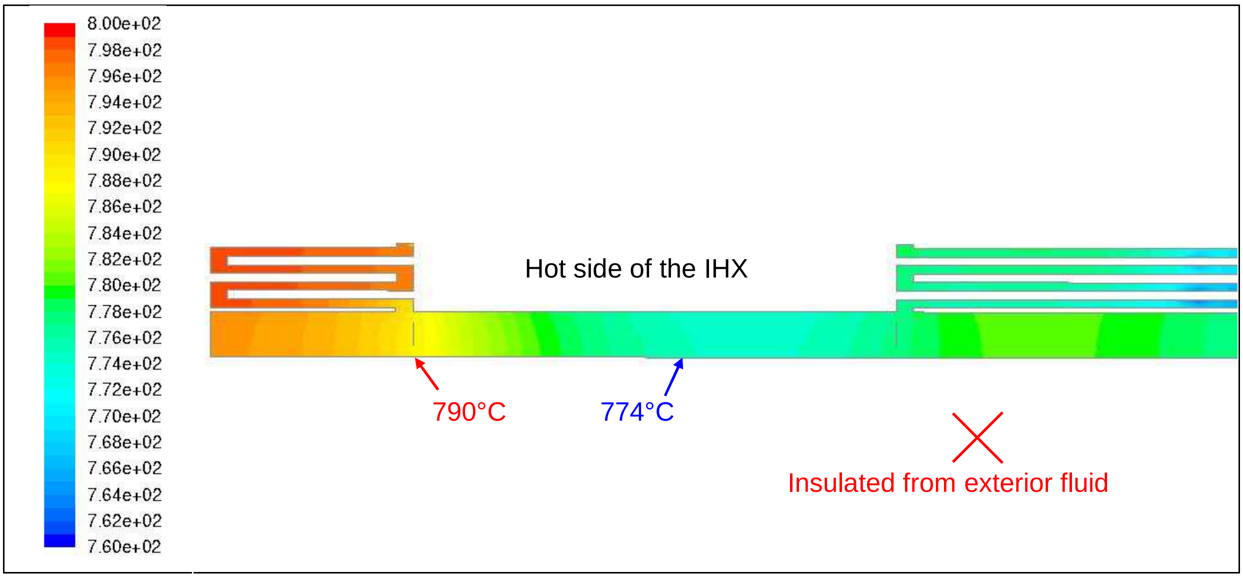

Figure 13 : Temperature longitudinal field with the collector in the hot part of the mock-up

Figure 12 and 13 show that the highest temperature difference in this area is not reached in the bottom end whereas it is the case for the IHX. .

For air-air mock-up which is insulated from external fluid, **temperature difference in the bottom end plate is 16°C only.**

Confidentialité : Les informations contenues dans le présent document sont la propriété des contractants. Ce document ne peut être reproduit ou transmis à des tiers sans l'autorisation expresse des contractants.

Imp 113 C

III.2.4 Conclusions for steady state

As assumed, half channels and end plates at each side of the IHX and mock-up affect temperature profile inside the heat exchanger even in steady state. They can't be neglected to model thermo-mechanical strain inside the heat exchanger.

For He IHX, highest DT around outlet collector is 31°C on the corrugated plate3. The lowest DT is 21°C on the plate4. The DT on other plates tends to 27°C which is the value found with the "single plate geometry" for plates which stands for the middle plates of the heat exchanger.

→ For transient calculations, special attention will be focussed on corrugated plate 3, 4 and on the bottom end plate.

For the air-air mock-up, DTs around outlet collectors are about 7°C lower than for the He-IHX. But temperature level is willingly 50°C higher. Based upon previous studies, we may hope those phenomenon are balancing themselves in order to generate equivalent thermo-mechanical effects.

The only major difference is on the bottom end plate where DT is 16°C for the air-air mock-up against 35°C for He-IHX, mainly due to external boundaries which are applied (Hot side of the IHX is immerged in hot primary helium whereas the mock-up is thermally insulated).

Confidentialité : Les informations contenues dans le présent document sont la propriété des contractants. Ce document ne peut être reproduit ou transmis à des tiers sans l'autorisation expresse des contractants.

III.3 Transient state simulations

III.3.1 « Full plate geometry », He-IHX

The figure 14 shows inlet hot fluid and outlet cold fluid temperature evolution during cold and hot shocks. The maximum DT around collector of corrugated plate3 is also plotted.

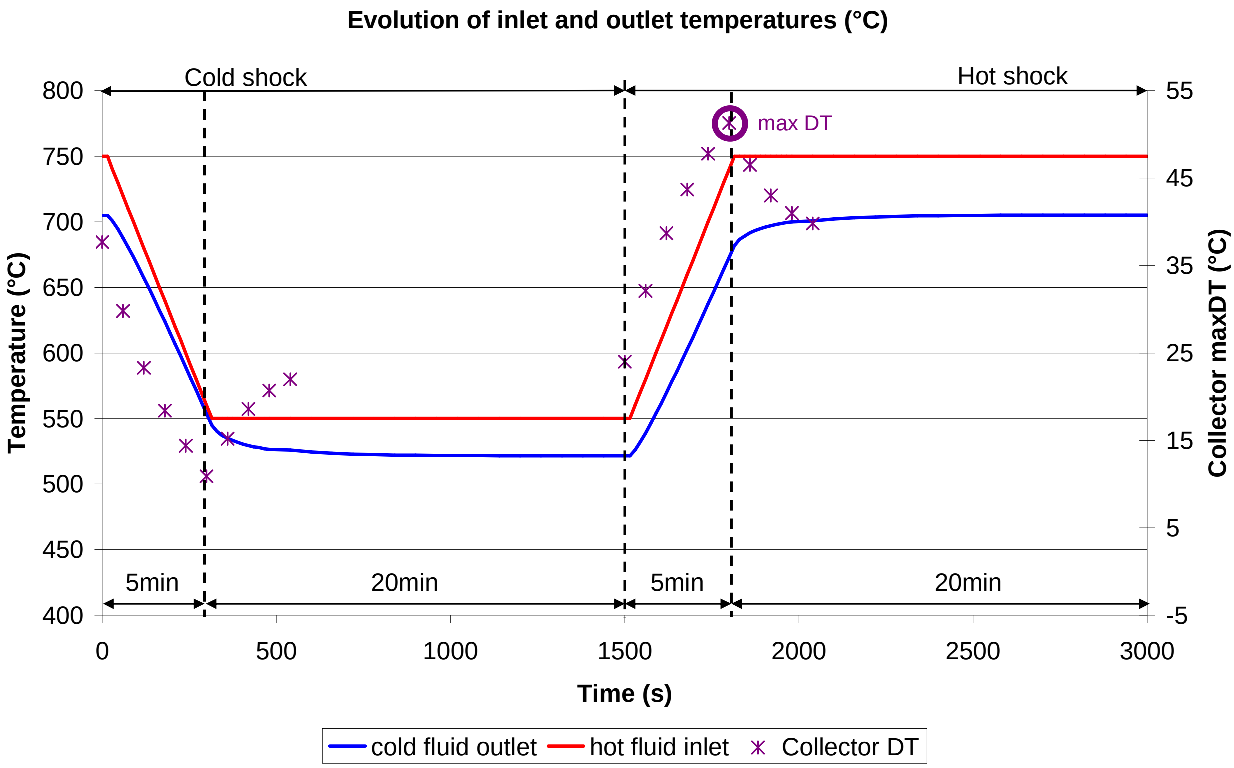

Figure 14 : Temperature evolution during hot and cold shocks

The profile of outlet cold fluid temperature follows the profile of inlet hot fluid temperature with a delay due to the thermal inertia of the IHX. This leads to a minimum and a maximum pick on the max DT around collector. This maximum is reached at the end of hot shock at 30min.

On figure 15, temperature profiles on left side and local temperature gradient profiles on right side are plotted during cold and hot shocks.

Confidentialité : Les informations contenues dans le présent document sont la propriété des contractants. Ce document ne peut être reproduit ou transmis à des tiers sans l'autorisation expresse des contractants.

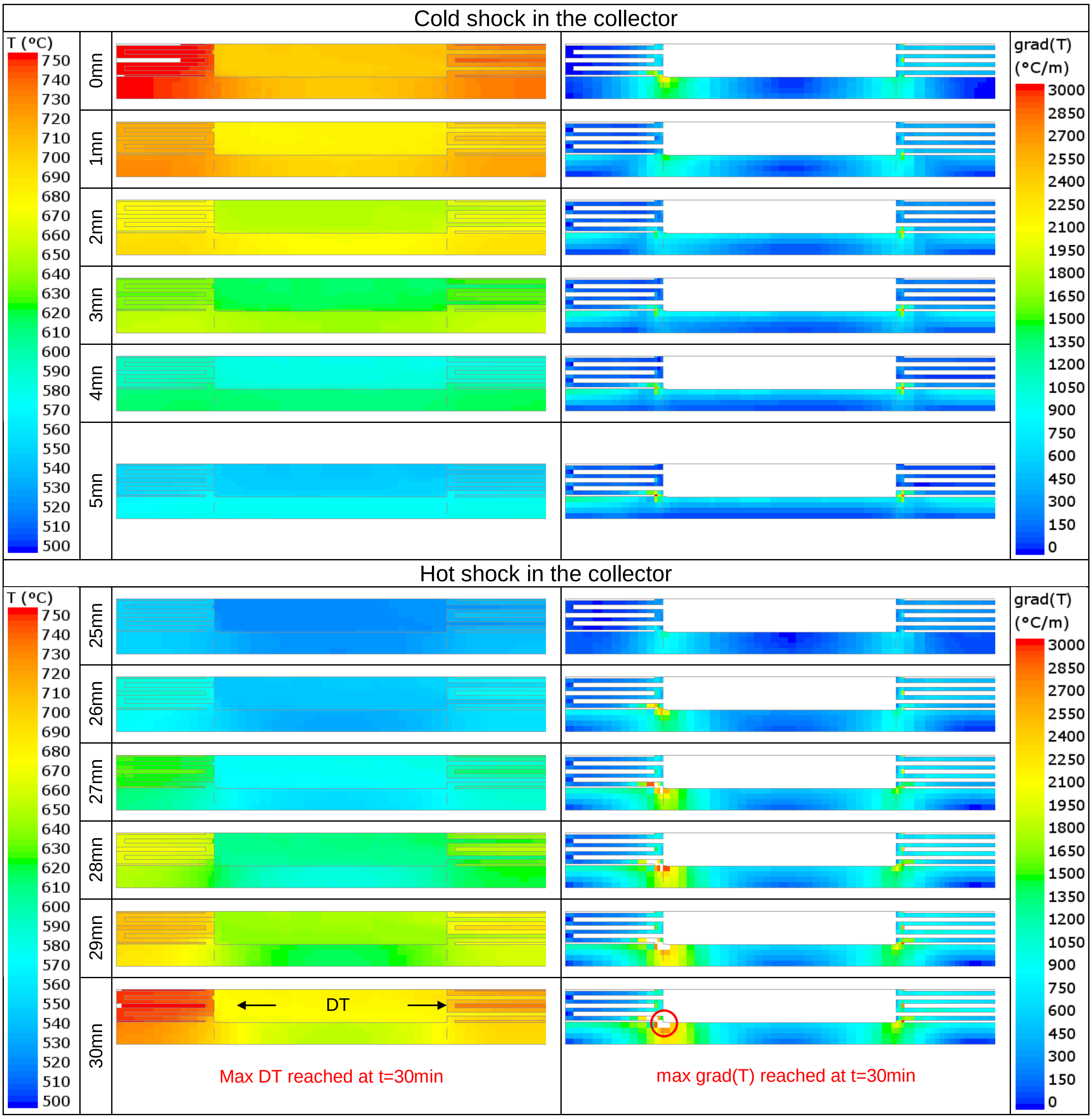

Figure 15 : Absolute temperature and gradient of temperature obtained during hot and cold shocks in IHX

Thermal inertia of the outer plate highly impacts thermal behaviour of the IHX during cold and hot shocks. Highest local temperatures and temperature gradients are reached at the end of hot shock at 30min; temperature gradients are concentrated on the welding between superior plate and plate4. Max grad(T) > 3000°C/m.

On figure 16, we represent plate3, plate4 and superior plate temperature fields at beginning and end of cold and hot shock only. Notice that temperature scale is adjusted at each time-step.

Confidentialité : Les informations contenues dans le présent document sont la propriété des contractants. Ce document ne peut être reproduit ou transmis à des tiers sans l'autorisation expresse des contractants.

Imp 113 C

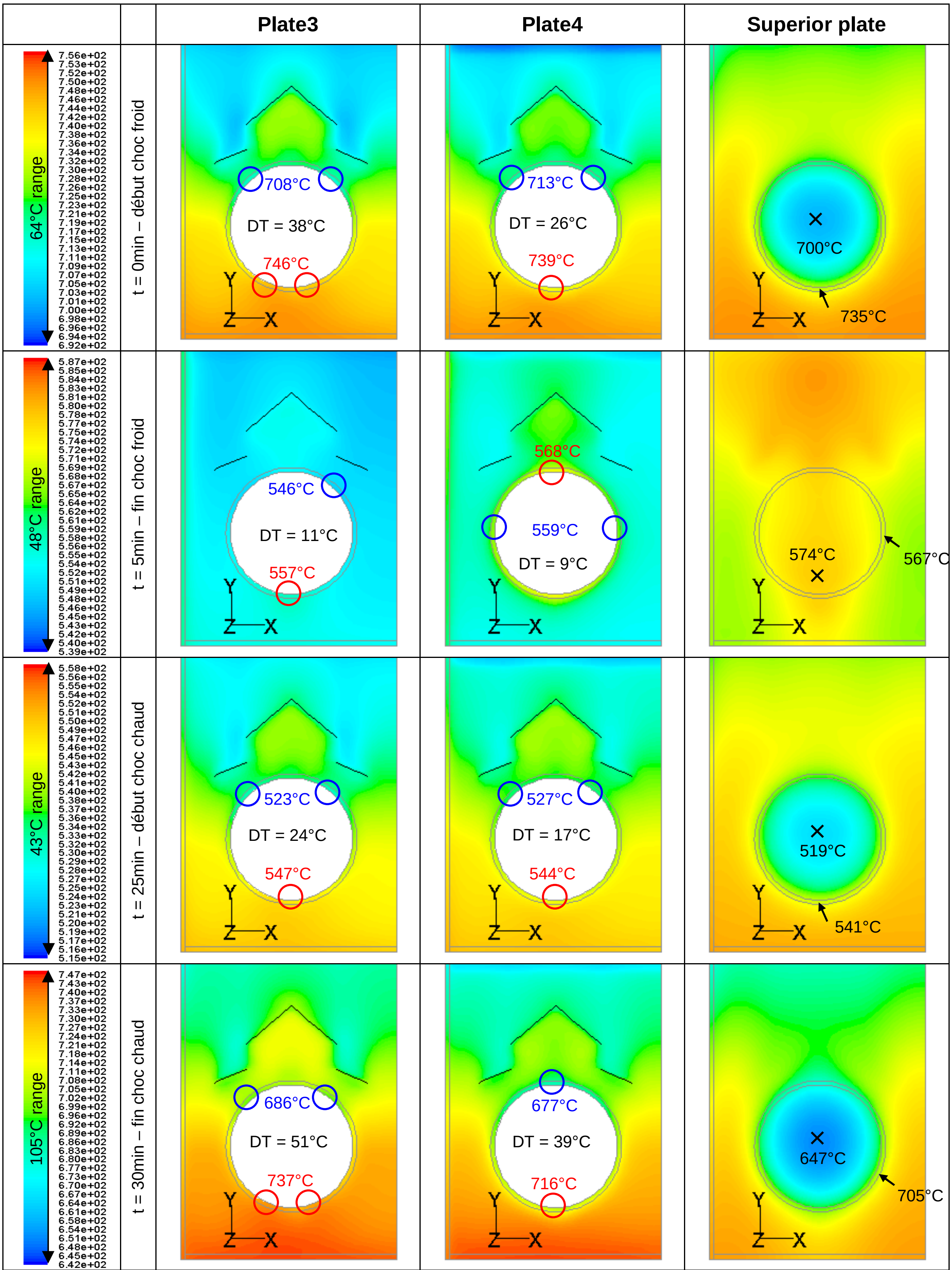

Figure 16 : Visualisation of temperature fields within plates during the shocks

Confidentialité : Les informations contenues dans le présent document sont la propriété des contractants. Ce document ne peut être reproduit ou transmis à des tiers sans l'autorisation expresse des contractants.

III.3.2 « Full plate geometry », air – air mock-up

The figure 17 shows the inlet hot fluid and outlet cold fluid temperature evolution during cold and hot shocks. The maximum DT around collector of corrugated plate3 is also plotted.

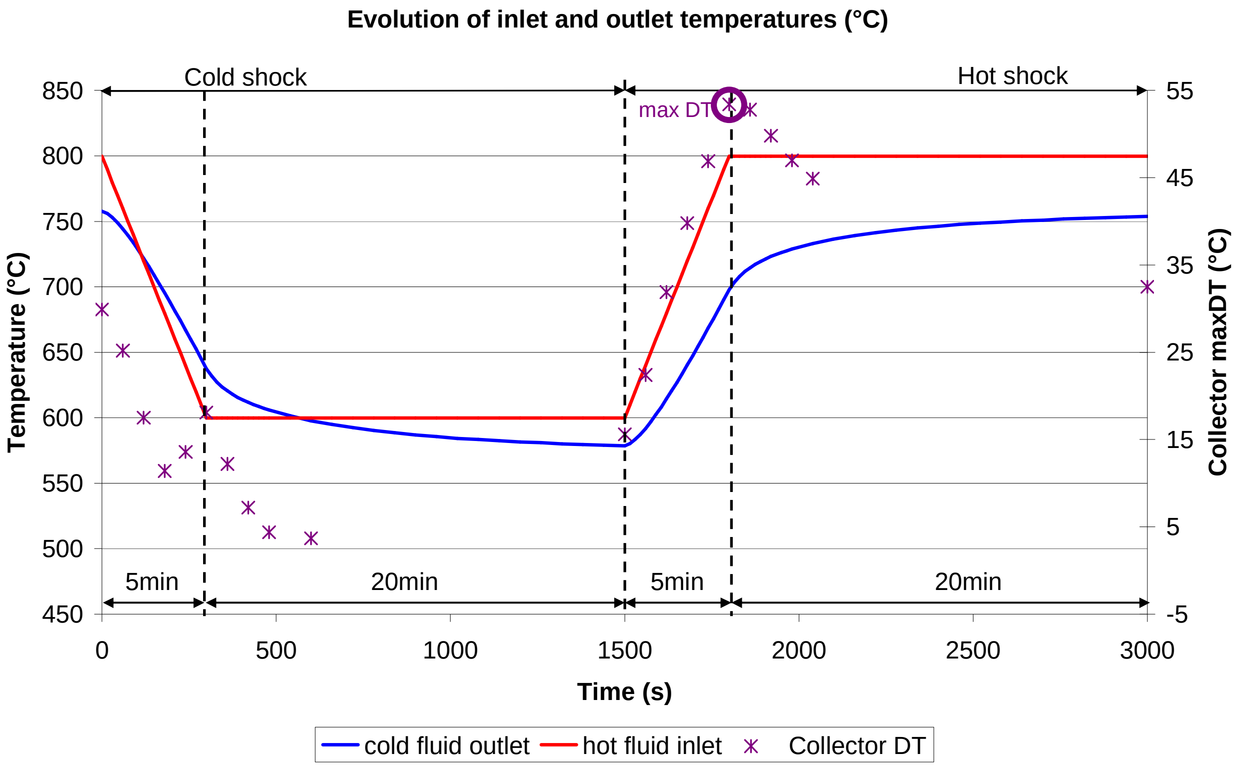

Figure 17 : Temperature evolution the mock-up of during hot and cold shocks

As in he-he simulation, the maximum collector DT is reached at end of hot shock at 30min.

In air-air configuration, the transient time is longer than in he-he due to thermal properties of air and external conditions (insulated air-air mock-up).

On figure 18, temperature profiles on left side and local temperature gradient profiles on right side are plotted during cold and hot shocks.

Confidentialité : Les informations contenues dans le présent document sont la propriété des contractants. Ce document ne peut être reproduit ou transmis à des tiers sans l'autorisation expresse des contractants.

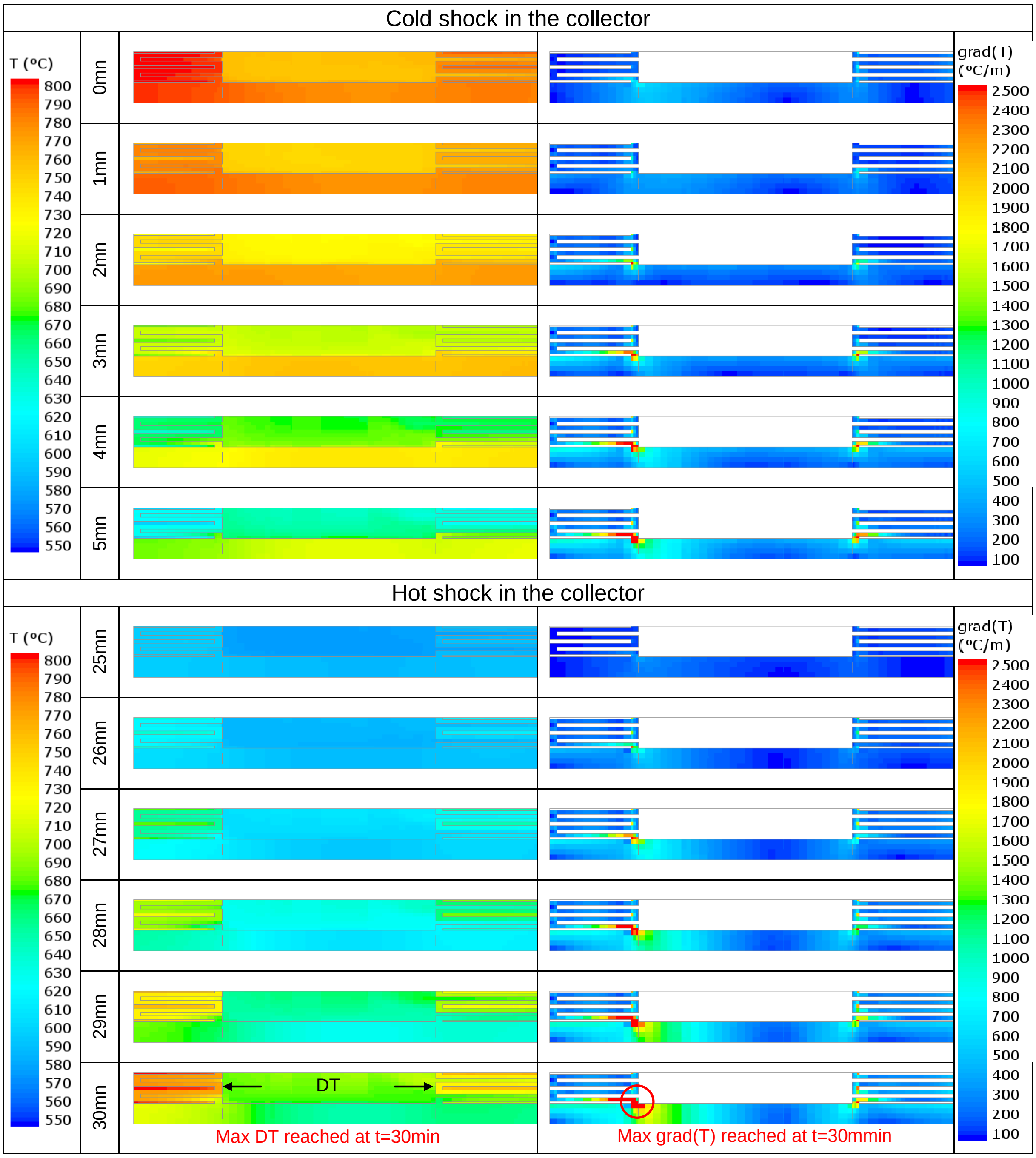

Figure 18 : Absolute temperatures and gradient of temperature obtained during hot and cold shocks in air-air mock up

The maximum thermal gradient is also reached at 30 minutes. The maximum gradient of temperature is around 2500°C/m instead of 3000°C/m in the IHX.

On figure 19, we represent plate3, plate4 and superior plate temperature fields at beginning and end of cold and hot shock only. Notice that temperature scale is adjusted at each time-step.

Confidentialité : Les informations contenues dans le présent document sont la propriété des contractants. Ce document ne peut être reproduit ou transmis à des tiers sans l'autorisation expresse des contractants.

Imp 113 C

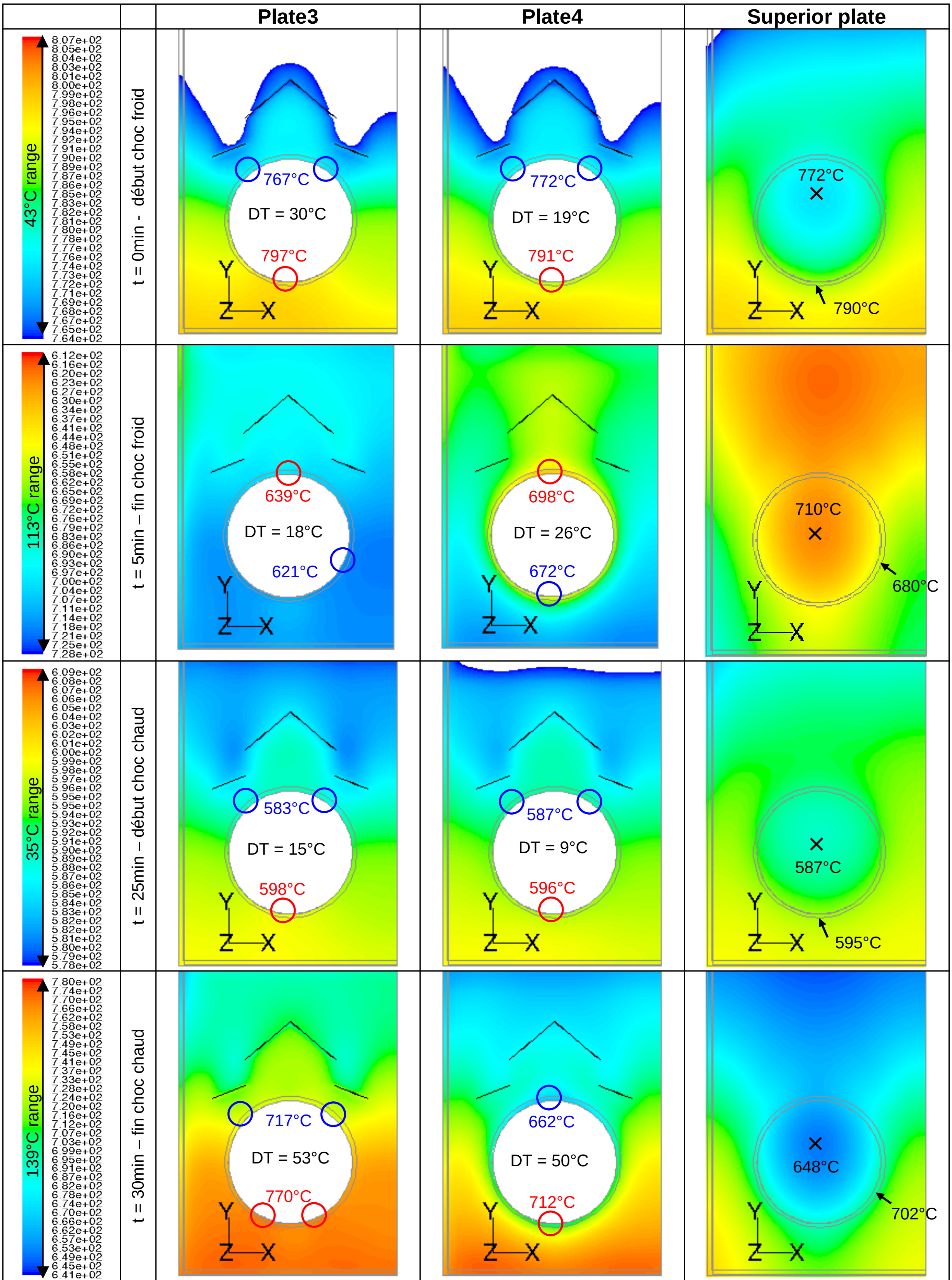

Figure 19 : Visualisation of temperature fields in the plate during the shocks

Confidentialité : Les informations contenues dans le présent document sont la propriété des contractants. Ce document ne peut être reproduit ou transmis à des tiers sans l'autorisation expresse des contractants.

Table 8 summarize DT around outlet hot side collector of plate 3 and 4 at t=0min and t=30min.

DT around outlet collector (°C)		**Plate3**	**Plate4**
t=0min	air-air mock-up	30	19
	he-he IHX	38	26
t=30min	air-air mock-up	53	50
	he-he IHX	51	39

Table 8: Main results of both geometries in transient state conditions for a full plate geometry

III.3.3 Conclusions for transient time calculations:

In transient conditions, i.e. during hot and cold shocks, it is necessary to model a stack of plates since the results are impacted by thermal inertia of the end plates. Depending on the boundary conditions applied on these plates, the results may be impacted: IHX is immerged in primary hot helium at the hot side whereas the air-air mock up is thermally insulated.

During cold and hot shocks, modelling of thermal inertia of end plates is necessary to thermo-mechanical strain calculations. Looking at plate 3 which is the most critical plate in steady state, it comes out:

- Cold shock tends to decrease the DT around the collector: starting from DT issued from steady state conditions this difference of temperature decreases both devices.
- Hot shock generates a different behaviour since DT around the collector increases to reach the same order of magnitude whatever the fluid is.
- So looking at plate3, the most critical phase is the hot shock and the maximum temperature difference around the collector is reached at the end of the shock.

Looking at welding between plate 4 and outer thick plate, maximum thermal gradient are generated at the end of the hot shock for both devices.

CFD calculations provide information concerning thermal and hydraulic performances which can be reached with IHX in helium conditions and with mock up in air conditions. These data are issued

Confidentialité : Les informations contenues dans le présent document sont la propriété des contractants. Ce document ne peut être reproduit ou transmis à des tiers sans l'autorisation expresse des contractants.

from simulations run with a single plate assuming perfect fluid flow distribution. These data may be used for FEM calculations considering the middle plates of a heat exchanger.

To go further with analysis, it is necessary to consider thick end plate and a stack of plates: a full plate geometry was modelled. Even in steady state conditions, temperature differences between plates are obtained since we have to take into account thermal conditions which are applied outside of the outer plate.

Transient conditions were also applied to this second geometry for he-he IHX and for air-air mock-up. Showing similar thermal behaviour between both devices, it is necessary to run FEM calculations. All the data are transferred to partners to carry out this task.

Confidentialité : Les informations contenues dans le présent document sont la propriété des contractants. Ce document ne peut être reproduit ou transmis à des tiers sans l'autorisation expresse des contractants.

3 Contribution from Alfa Laval Packinox

IHX-Finite Element Analysis-2012

-Alfa Laval Packinox-

REVISION Version	Nom *Name*	Entité *Entity*	Date *Date*
Rédacteur *Writer*	BENGUERGOURA Mohamed Seddik	Mechanical department	23/11/2012
Vérificateur(s) *Reviewer(s)*	Franck BAURAND	Mechanical department	14/12/12
Approbateur *Approver*	**Alain BOURGEON Pierre-Xavier BUSSONNET**	Mechanical department	17/12/12

SUMMARY

1. Subject

The objective of this report is to summarize the results of the finite element analysis(the study of year 2012 for Alfa Laval Packinox) of Intermediate Heat Exchanger "IHX" in the following cases:

With Incoloy 800H material: (the material currently used for IHX module)

- In Transient conditions

With Inconel 617 material: (this study is given for information because the Inconel 617 material is no longer used for IHX module)

- In Steady State conditions
- In Transient conditions

All these calculations take into account the thermal inertia of the external plate. The calculations are done using the finite element method in the SYSTUS software version 2010.

2. Modeling

The structure is modeled using volume elements composed of 8 nodes. The model has 43264 nodes and 42042 elements. It was meshed using SYSTUS software.

The figures 1 present the finite element model.

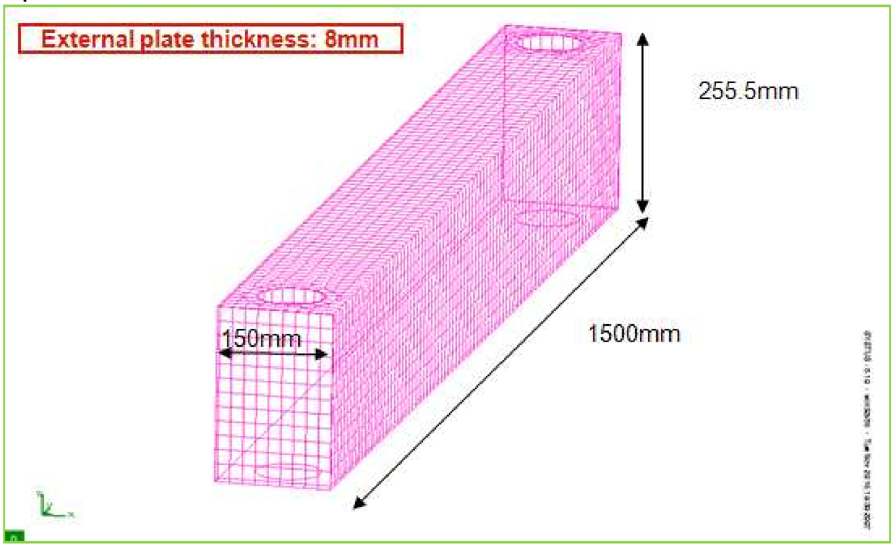

Figure 1 - Mesh of ¼ exchanger

3. Material characteristics

The material characteristics are used as follows:

- Equivalent orthotropic material behavior and independent of temperature for bundle (presented by red color on figure 2)
- Real material behavior for external plate, wall and the ends of channels using a unified viscoplastic model type Armstrong - Frederick (presented by blue color on figure 2) for Inconel 617 case.
- Real material behavior for external plate, wall and the ends of channels for 800H material case.
- Poisson's ratio: Nu=0.3
- Coefficient of thermal expansion: $15*10^{-6}$ ℃ $^{-}$

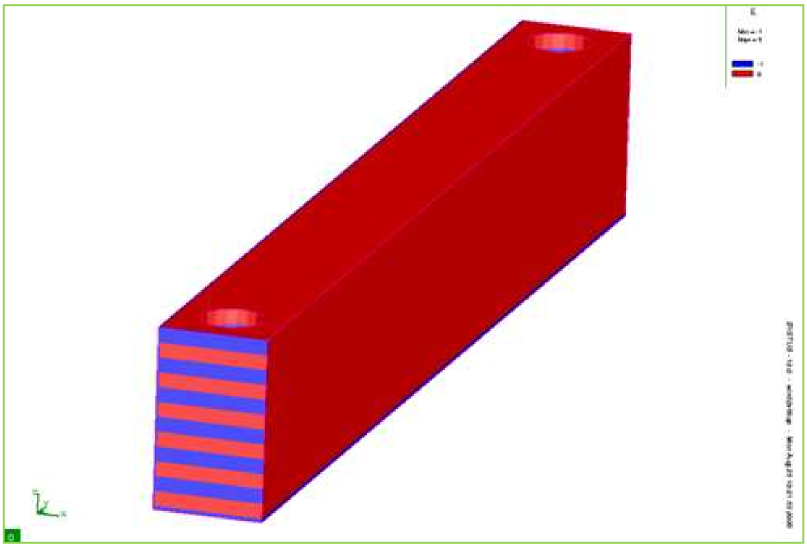

Figure 2 - material characteristics

4. Boundary conditions

To respect to the symmetry of the model, the following boundary conditions are applied:

- Blocking displacement in the Z direction of the vertical symmetry plane (in red On Figure 3),
- Blocking displacements along the X direction of the horizontal symmetry plane (in blue on Figure 3),
- Blocking all degrees of freedom of one node to neutralize the movement of rigid bodies.

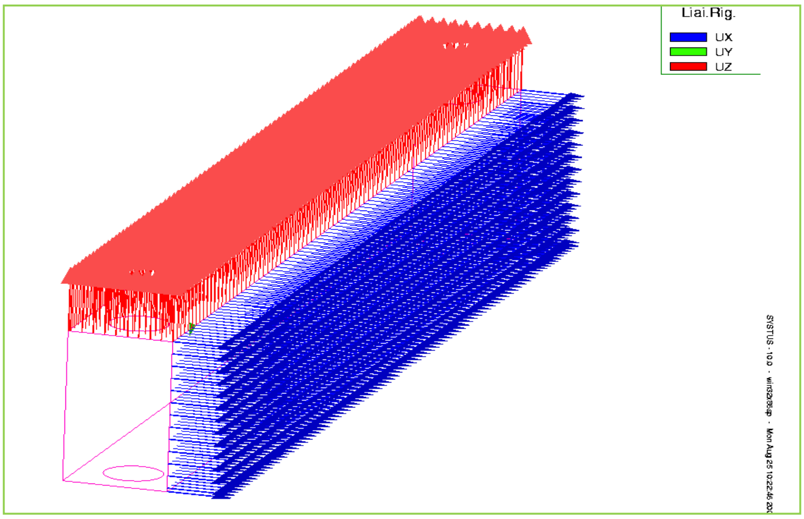

Figure 3 - boundary conditions

5. Steady state calculation with Inconel 617

Only for information we have included the results of calculation with material Inconel 617. In fact, this material is no longer the material used for IHX module. The results of calculation with the material 800H (currently used) are presented after.
A thermal load corresponding to the start of the device has been imposed. This loading will increase the temperature of the primary fluid inlet from 50 °C to 750 °C in about 30 hours with a series of successive steps, while the temperature of the secondary fluid inlet is changing from 20 °C to 300 °C in the same time.
We consider that we have a steady state at the end of the second stage.

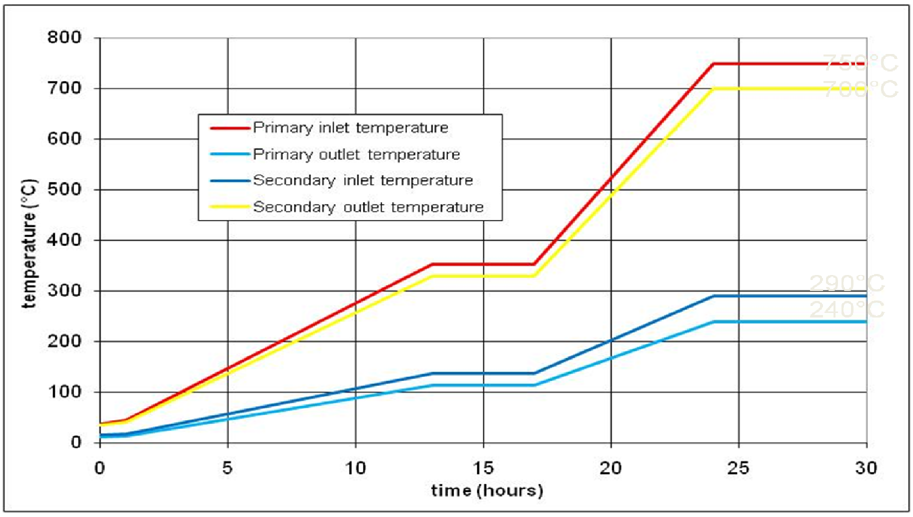

Figure 4 - Thermal load

5.1. Temperature field

The temperature gradient applied on the heat exchanger is the result of a calculation in fluent. Temperatures are then interpolated for the external plate and first four metal sheets. Consequently ,there is a vertical temperature gradient through the external plate and the first four metal sheet.
For the rest of the structure we take the fourth plate temperature.

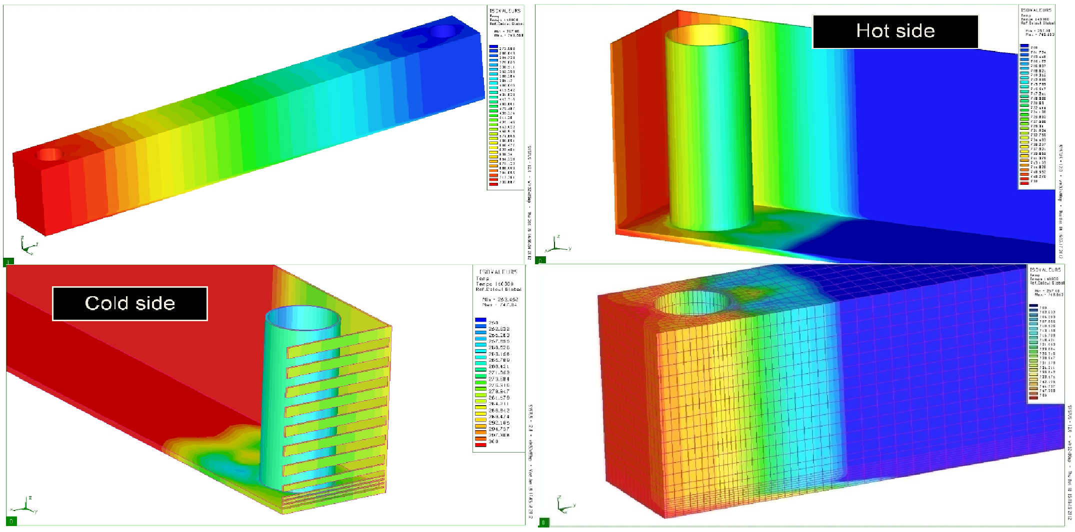

Figure 5 – Temperature field

5.2. Von Mises Stress

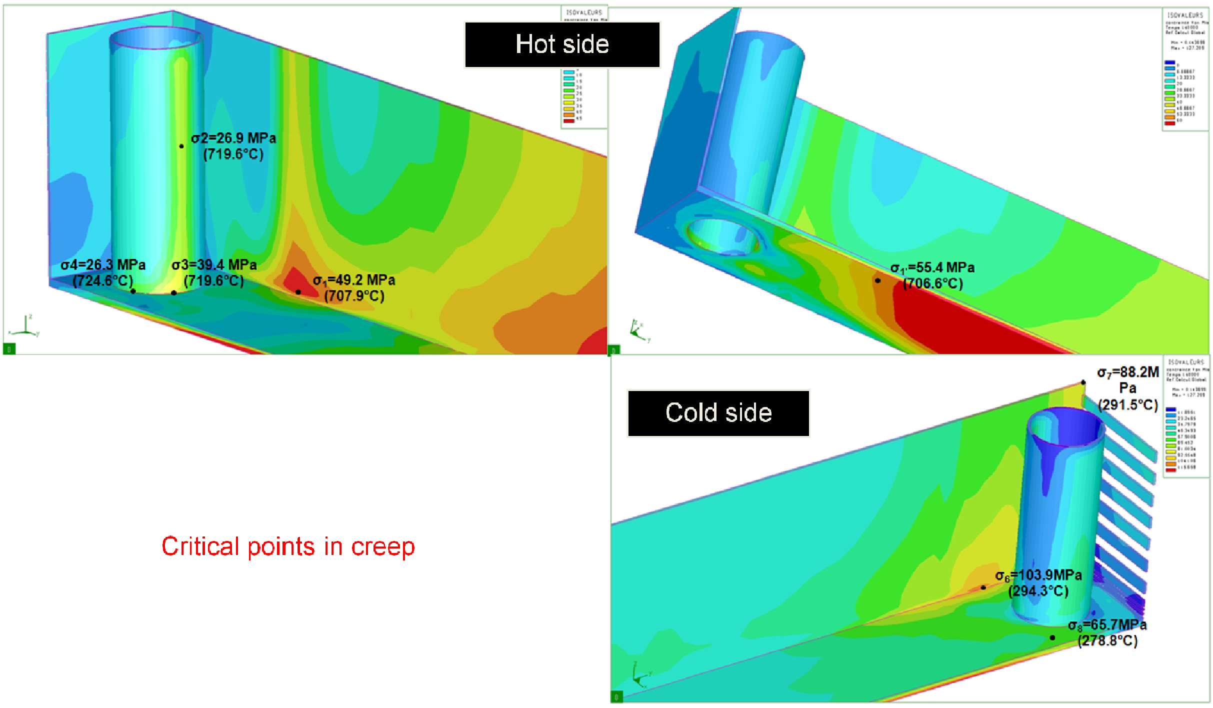

Figure 6 – Von Mises Stress

In this thermo-elastic calculation we take into account the effect of creep, so we had identified the most critical points according to their temperatures and their stress.

5.3. Analysis creep

Thermal data with external plate inertia								Thermal data without external plate inertia			
stress n°	side	position	Temperature	Stress	Life time			Temperature	Stress	Life time	
			°C	MPa	h	year		°C	MPa	h	year
1	hot	external plate	707.9	49.2	164 357	18.8		710.5	51.9	126 076	14.4
1'		external plate	706.6	55.4	109 858	12.5					
2	hot	collector middle	719.6	26.9	648 000	74.0		721.5	27.2	611 444	69.8
3	hot	collector basis	719.6	39.4	247 969	28.3		721.4	48.6	116 142	13.3
4	hot	collector basis	724.6	26.3	620 478	70.8		719.6	32.3	428 167	48.9
								744.7	23.5	537 840	61.4
6	cold	external plate	294.3	103.9	$>10^6$	$>10^6$		277.3	108.5	$>10^6$	$>10^6$
7	cold	collector basis	291.5	88.2	$>10^6$	$>10^6$		285.8	63.2	$>10^6$	$>10^6$
8	cold	corner	278.8	65.7	$>10^6$	$>10^6$		272.3	66.7	$>10^6$	$>10^6$

Figure 7 – comparative table of lifetime in creep

In this table we find a comparison between the current results **with** the external plate inertia and the previous results **without** the external plate inertia , we can see that we have practically the same critical zones and points with approximately the same lifetime . On the cold side we still having a infinite lifetime but on the hot side, we note the appearance of a new critical point P1 ' situated on the external plate, caused by the application of a temperature gradient on the external metal sheet.
We also note that the point 3 (located between the bottom of the collector and the external sheet) is no longer the most critical point because its temperature has decreased.

In terms of creep, the lifetime of the heat exchanger has decreased from 13.3 years to 12.5 years and this is due to the application of temperature gradient on the external plate and the first four metal sheets.

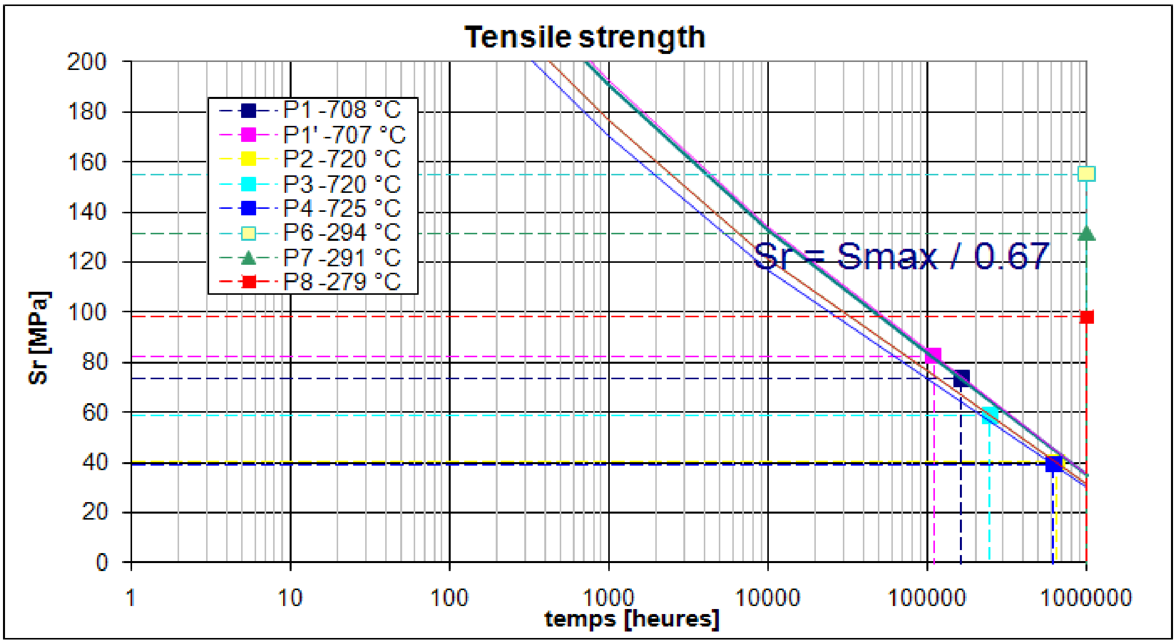

Figure 8 – Creep curve - lifetime: 109 858h=12.5 years

6. Transient calculation with Inconel 617

Now we are studying the structure in transient conditions, we keep the same geometry and we applied the same boundary conditions presented previously.
The thermal load is applied by controlling the inlet of primary helium as the graph below
It's composed by:

- A cold shock : a loss of 200 °C at the primary inlet in 4 minutes (DT/dt = -50 ℃ /min)
- A hot shock : a gain of 200 °C at the primary in let in 5 minutes (DT/dt = +40 ℃ /min)

We note that the temperature at the secondary inlet is maintained at 340 ℃.
We consider 1000 occurrences in 20 years, or about 1 occurrence per week.

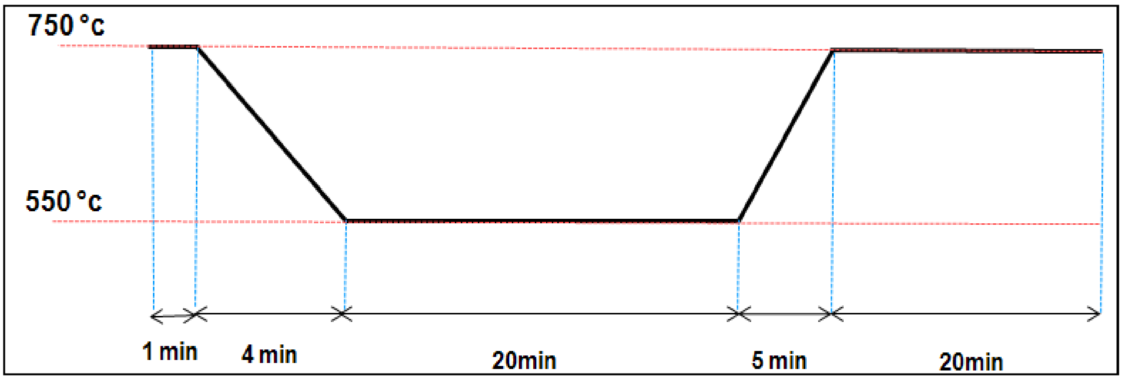

Figure 9 – Piloting of temperature at primary inlet

6.1. Evolution of temperature in the hot side

In the figure below we have the evolution of the temperature on the critical points identified previously in the steady state calculation. The temperature on these points follows the temperature imposed at the inlet of primary helium and we have clearly the hot and the cold shock.

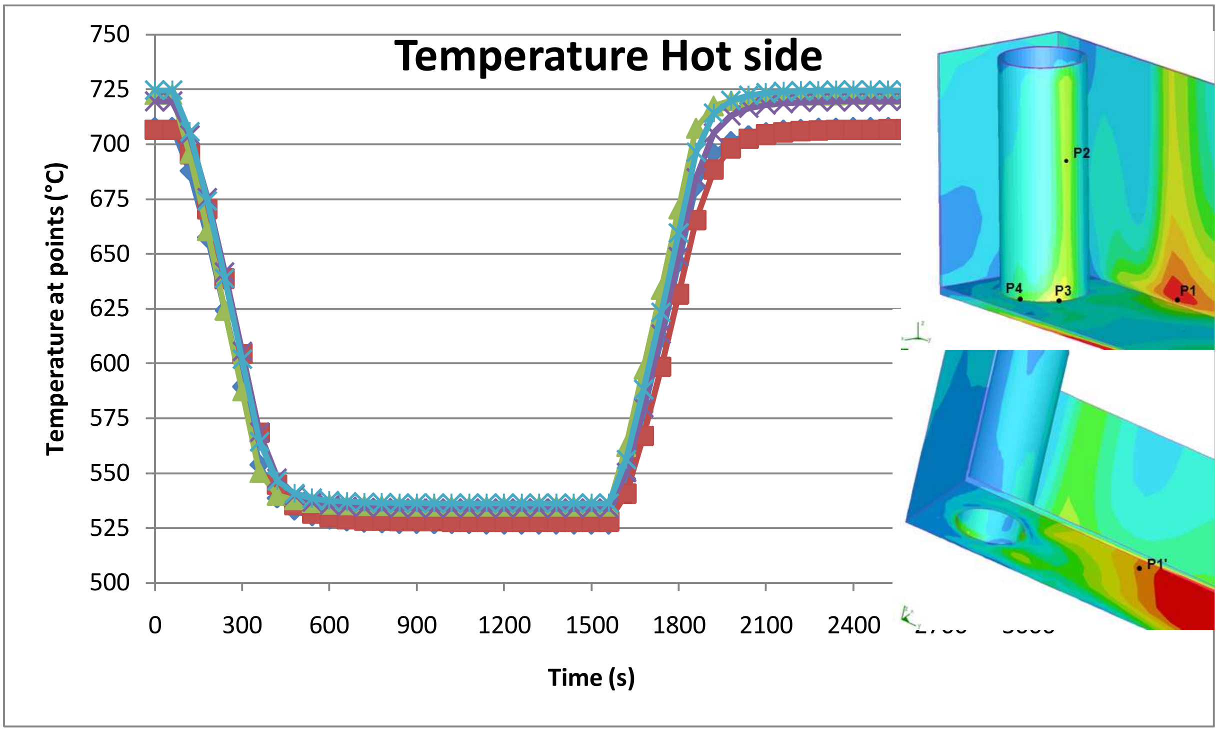

Figure 10 –Temperature hot side

6.2. Evolution of Von Mises stress in the hot side

In the graph bellow we have the evolution of Von Mises Stress depending on time of the hot side. We see that we have a maximum and minimum of stress during the cold shock and the hot shock .We find also that the largest stress amplitude is on the point P1 ' and P3, so we keep the same critical points as the steady state calculation.

We note also that we don't have the same sensibility on these critical points. In fact, on the point P1' we have a maximum of stress during the cold shock and a minimum of stress during the hot shock, but we have the opposite on the point 3, we have a minimum of stress during the cold shock and maximum of stress during the hot shock.

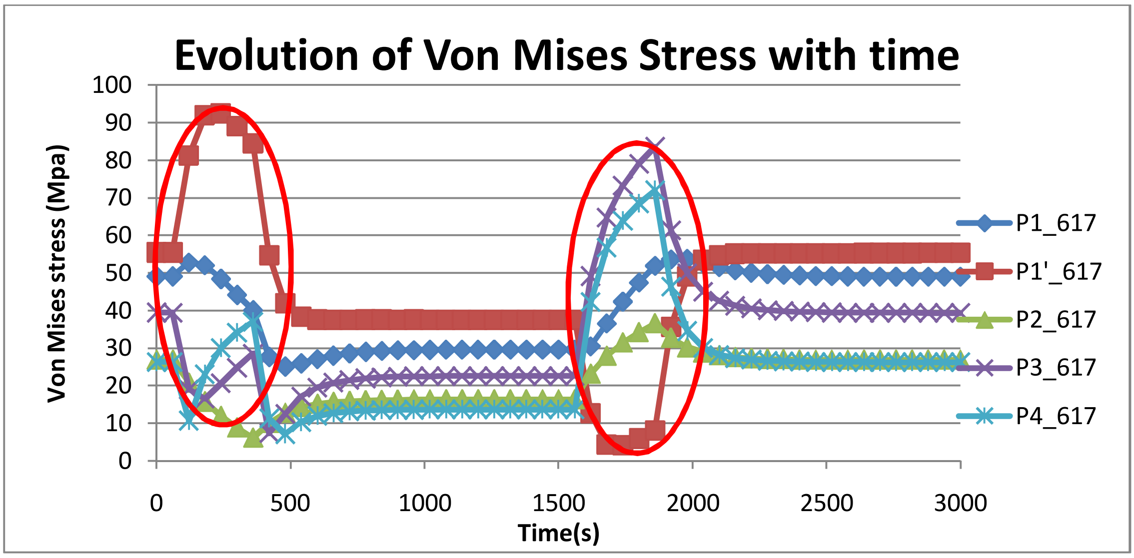

Figure 11 –Evolution of Von Mises Stress

In the figure 12, we have a comparison between the results of this calculation taking into account the thermal inertia of the external plate and the previous transient calculation without the thermal inertia of the external sheet .We can see that we had the point 8 as the most critical point, it is what we call today the point 3.So we have multiplied by 2 the stress on this point, and this is due to the application of temperature gradient particularly on the external plate.The maximum of stress it is on the point P1' during the cold shock, where we have 92 Mpa.

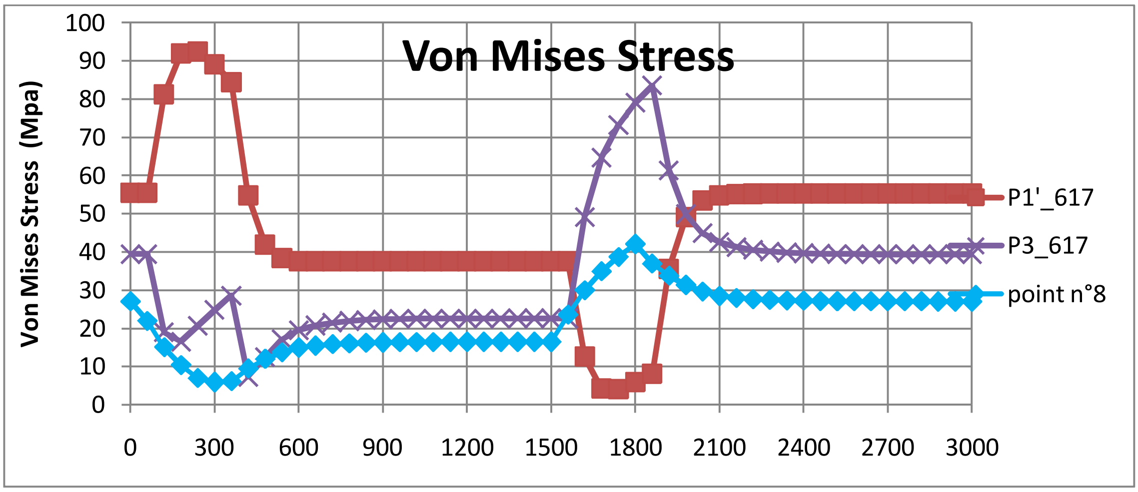

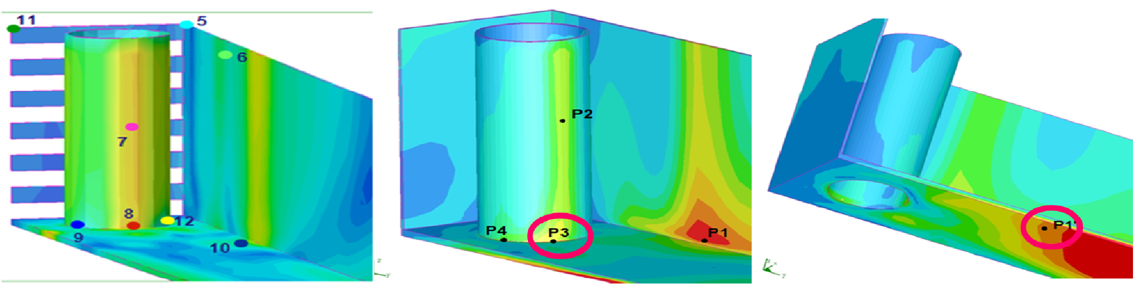

Figure 12 –Comparison of Von Mises Stress

6.3. Rupture Analysis

Concerning the rupture analysis, we use the graph below presenting the tensile strength of Inconel 617 depending on temperature (ref. Huntington Alloys). At 750 ℃, the maximum of temperature on the heat exchanger, the tensile strength of Inconel 617 is 482.6 Mpa .If we divide this tensile strength by the stress at point P1’ which is about 92.4 Mpa , we find that we have a factor of **5** as a safety margin in rupture.

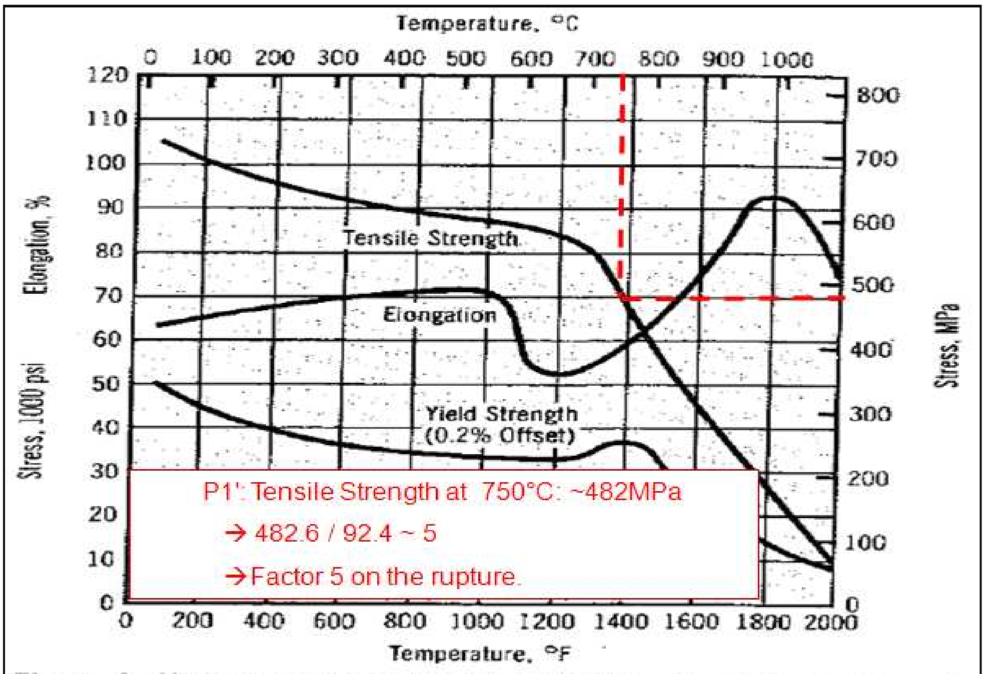

Figure 2. High-temperature tensile properties of solution-annealed, cold-rolled sheet.

Figure 13 –Tensile strength of Inconel 617

6.4. Fatigue Analysis

For fatigue analysis we use a fatigue curve at 10 000 cycles based on the total strain amplitude (ref. Huntington Alloys).We have therefore followed the procedure of ASME VIII div.2 to estimate a margin of safety in fatigue using the strain and stress tensors components of the points P1 ' and P3 (considered as the most critical point).On the figures below we have the strain and stress tensor components of the point P1’ and P3 during the transient calculation.

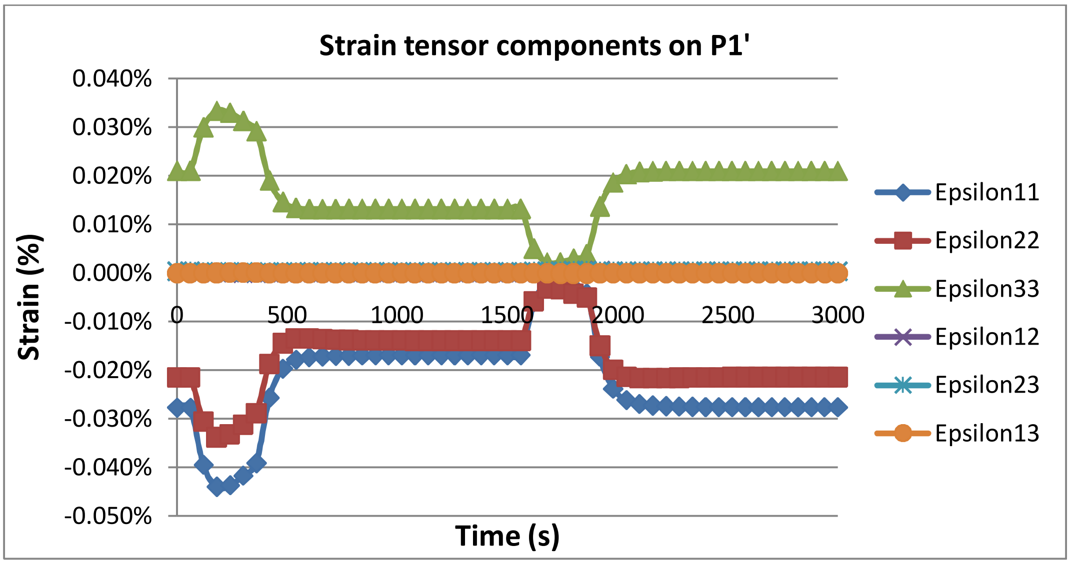

Figure 14 –Strain tensor on point P1' (617)

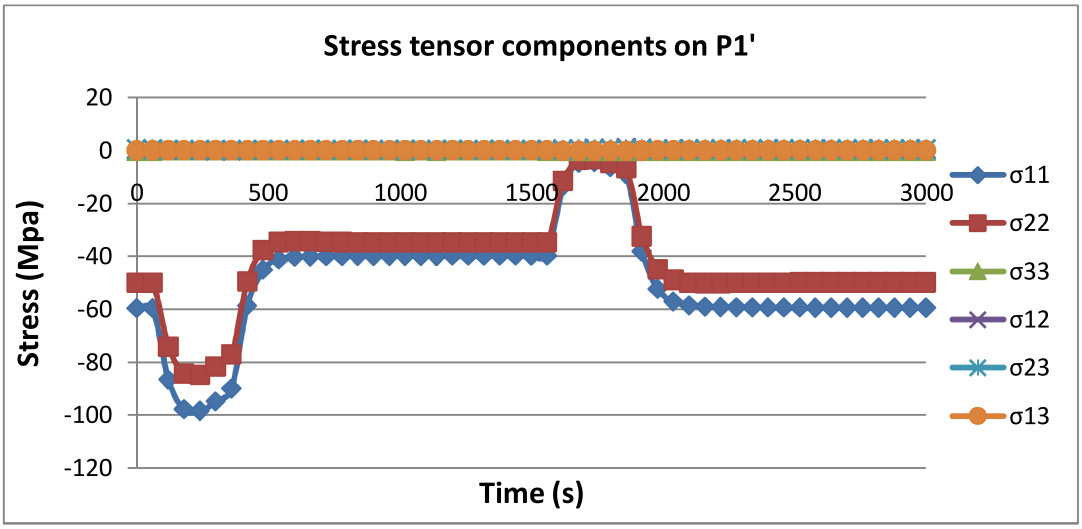

Figure 15 –Stress tensor on point P1' (617)

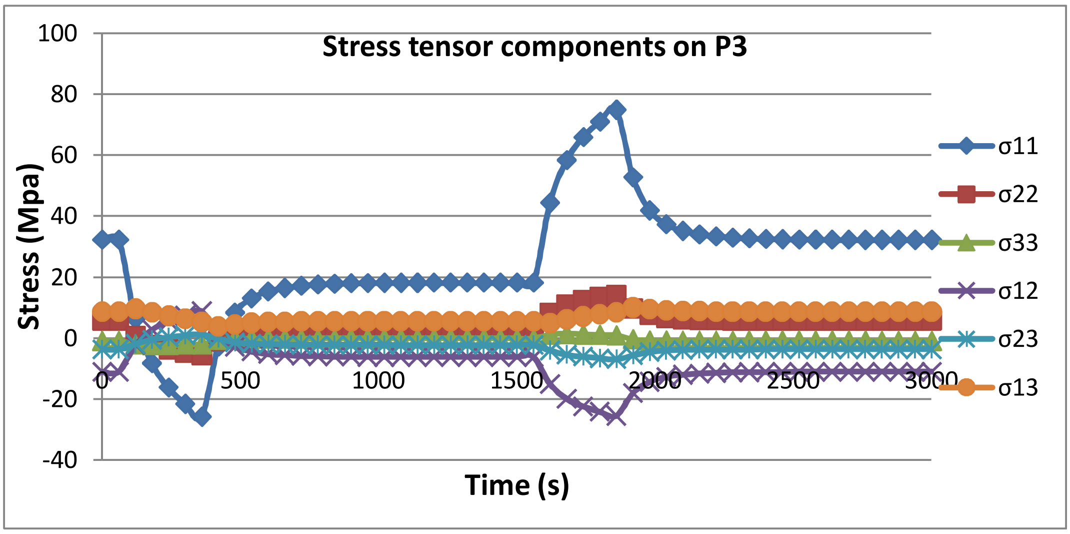

Figure 16 –Stress tensor on point P3 (617)

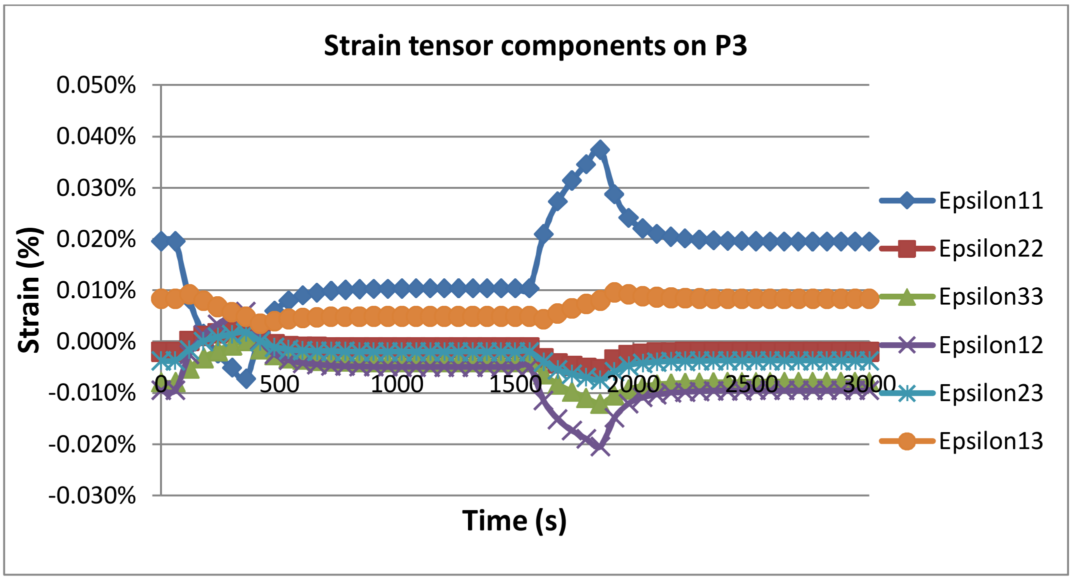

Figure 17 –Strain tensor on point P3 (617)

Calculation of the effective strain range$\Delta\varepsilon_{eff}$:

$$\Delta\varepsilon_{eff} = \frac{\Delta S_p}{E_{ya}} + \Delta\varepsilon_{peq}$$

Where the stress range ΔS_p is given by the equation:

$$\Delta S_p = \frac{1}{\sqrt{2}}\sqrt{(\Delta\sigma_{11}-\Delta\sigma_{22})^2+(\Delta\sigma_{11}-\Delta\sigma_{33})^2+(\Delta\sigma_{22}-\Delta\sigma_{33})^2+6\left(\Delta\sigma_{12}{}^2+\Delta\sigma_{13}{}^2+\Delta\sigma_{23}{}^2\right)}$$

The equivalent plastic strain range $\Delta\varepsilon_{peq}$ is given by the equation:

$$\Delta\varepsilon_{peq} = \frac{\sqrt{2}}{3}\sqrt{(\Delta\varepsilon_{11}-\Delta\varepsilon_{22})^2+(\Delta\varepsilon_{11}-\Delta\varepsilon_{33})^2+(\Delta\varepsilon_{22}-\Delta\varepsilon_{33})^2+1.5\left(\Delta\varepsilon_{12}{}^2+\Delta\varepsilon_{13}{}^2+\Delta\varepsilon_{23}{}^2\right)}$$

E_{ya} is the modulus of elasticity of the material Inconel 617 evaluated at the mean temperature on the considered point.

Then on point P1':

$$\Delta\varepsilon_{eff} = \frac{88.45}{172100} + 7.46^{-5} = 0.059\%$$

On point P3:

$$\Delta\varepsilon_{eff} = \frac{79.15}{171432} + 22.67^{-5} = 0.069\%$$

The fatigue curve below gives a total strain of 0.6% for a period of life corresponding at 10 000 cycles at 750°C. So we have a factor of about **10.2** (0.6%/0.059%) on strain at the point P1' to attain 10 000 cycles (knowing that we consider 1000 cycles / 20 years). Therefore we have a comfortable safety margin in fatigue on this point but we have a safety margin fatigue less comfortable on point P3, which is about a factor of **8.7**.

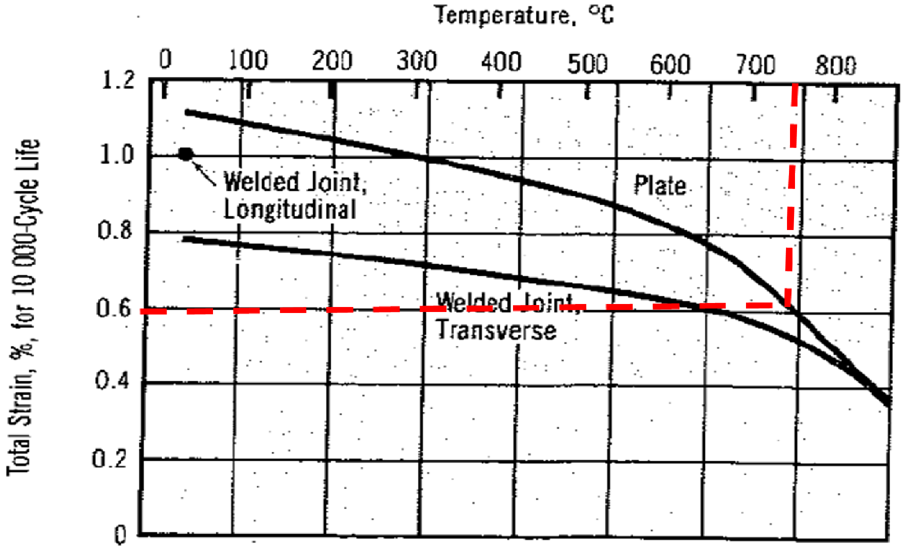

Figure 18 –Fatigue curve at 10 000 cycles of Inconel 617

6.5. Results of the cold side

For information we find in the figures below the evolution of temperature and strain on the cold side. In fact, in the steady state calculation these points are not an issue in terms of lifetime even if we have significant stress because their temperatures are low.

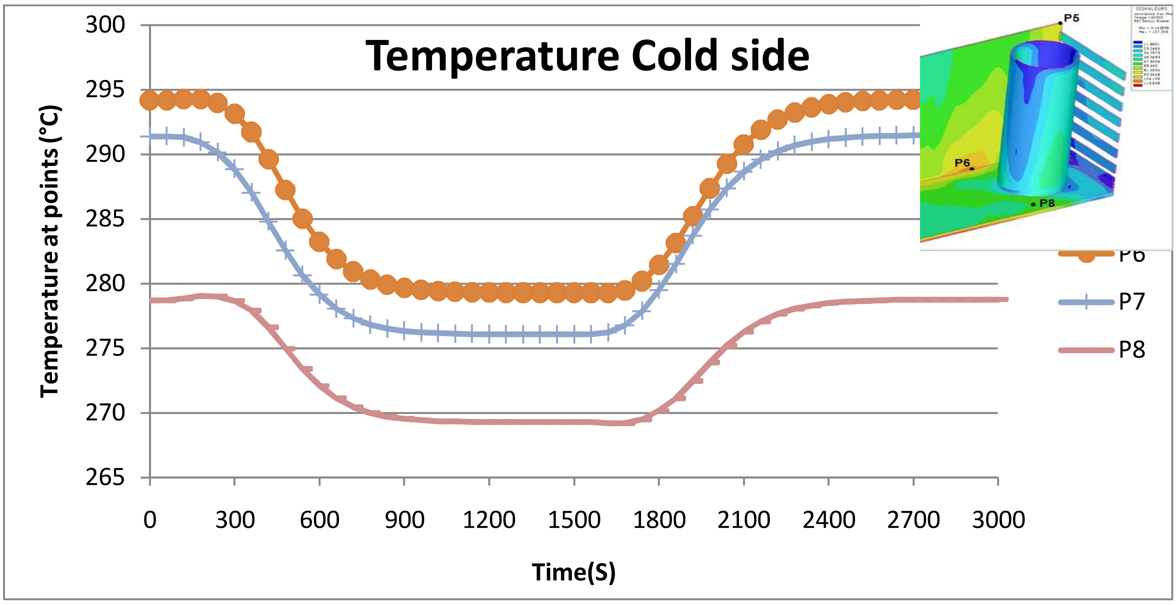

Figure 19 –Temperature in cold side

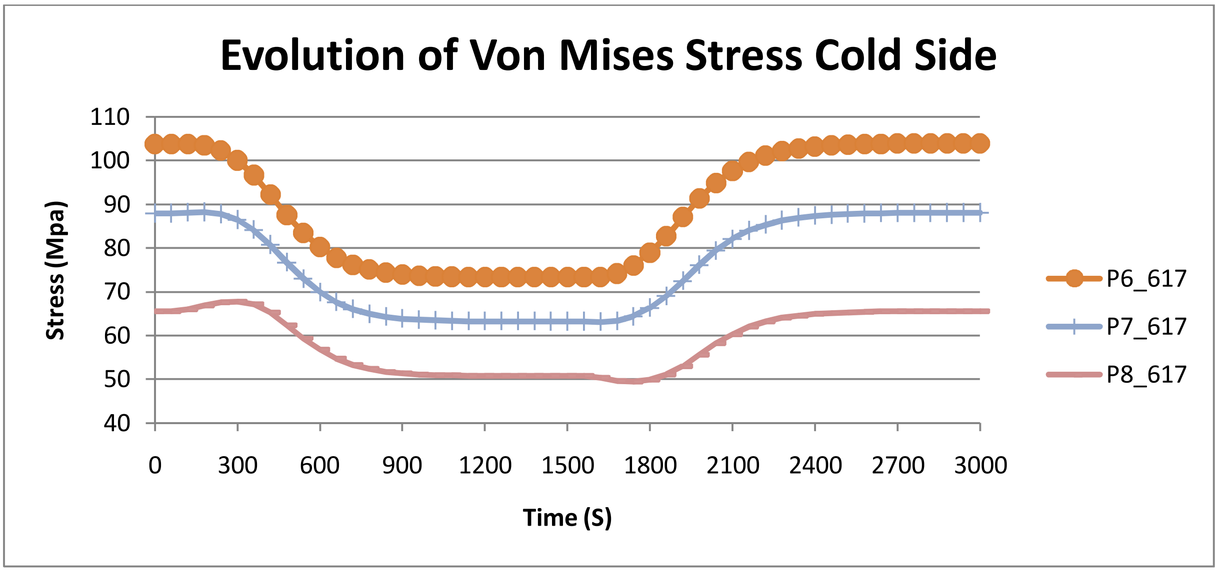

Figure 20 –Von Mises stress in cold side

7. Transient calculation with Incoloy 800H

7.1. Evolution of Von Mises stress in the hot side

In this chapter, we make a comparison between the model with the material Incoloy 800H and the model with material Inconel 617.The thermo-mechanical calculation is based on elastic behavior. The effect of creep is not included because the material characteristics in creep are not available yet (April2013).

The calculation taking into account the effect of creep will be a subject of a future study once the material characteristics in creep for the 800H will be provided. Given that the effect of creep is not significant ,this thermo-elastic calculation with 800H shows us that we have the same mechanical behavior in terms of Von Mises stress and critical zones , so we have the same critical points P3 and P1' .

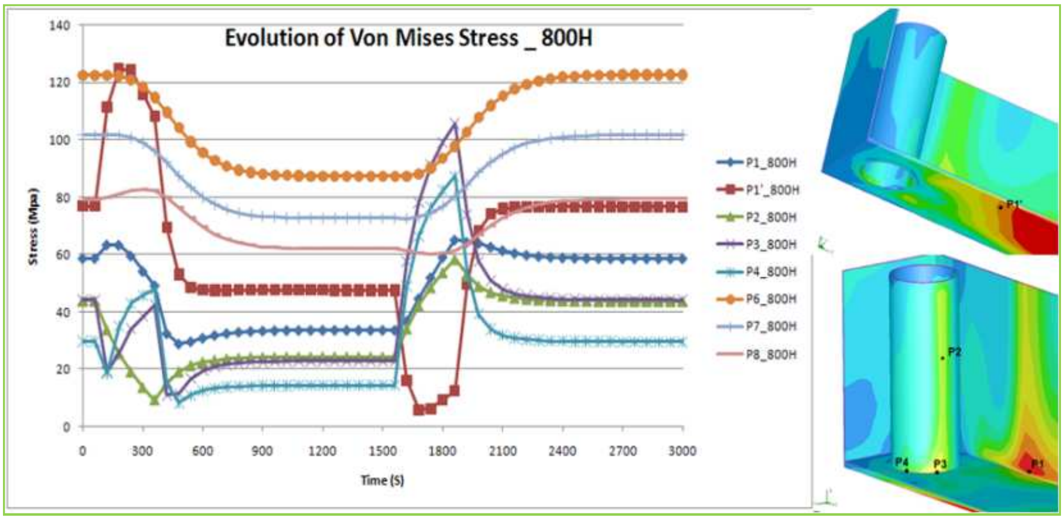

Figure 21 –Evolution of Von Mises stress (800H)

In the graph below, we have the evolution of the Von Mises stress of critical points P1' and P3, for both materials 617 and 800H.We see that the stress amplitude has increased on these points, which will have probably an impact in terms of a lifetime.

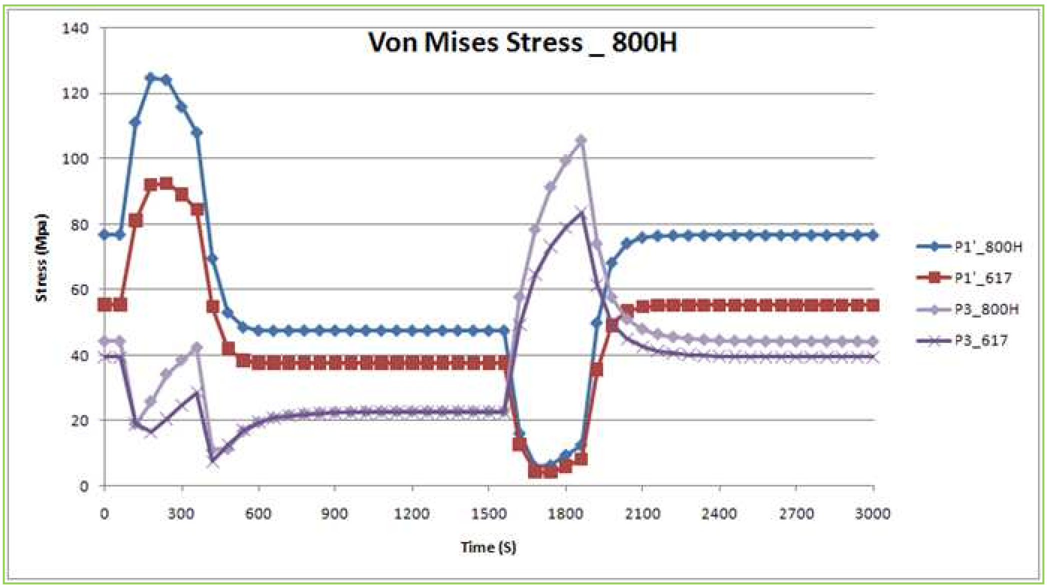

Figure 22 –Comparison of Von Mises stress (800H-617)

7.2. <u>Fatigue Analysis</u>

We have a fatigue curve of Incoloy 800H provided by the report from Alstom & Areva (ref.Areva.N° PEEL-F 2011 DC 145 / ref.Alstom.N° TN 11/1114), this curve is based on the total amplitude of strain depending on a number of cycles.
To make a comparison between the two materials 800H and 617, we take 10 000 Cycles at 750°C, at this number of cycles we have 0.2 % as m aximum allowable of strain range.

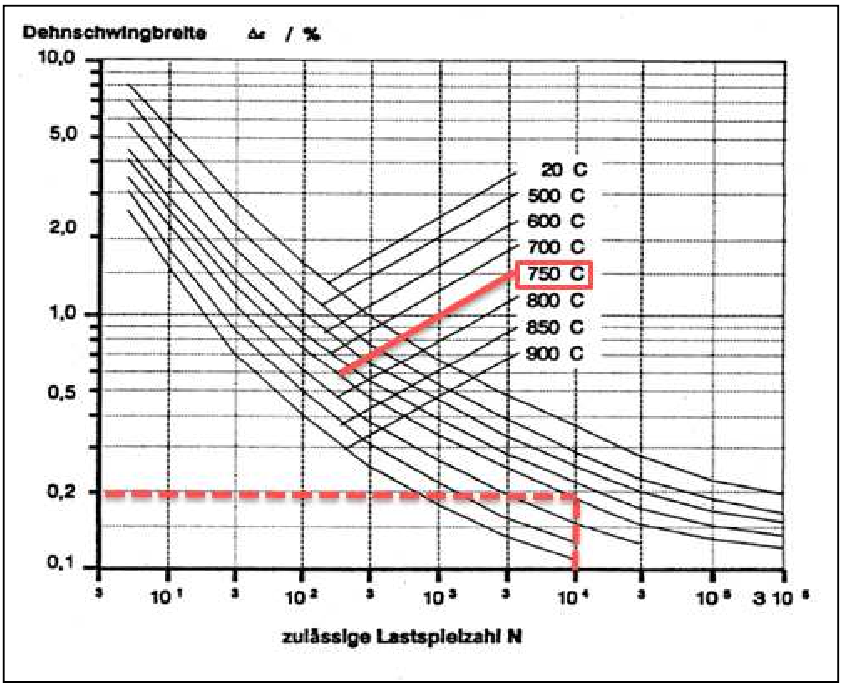

Figure 23 –Fatigue curve of Incoloy 800H (Alstom & Areva report)

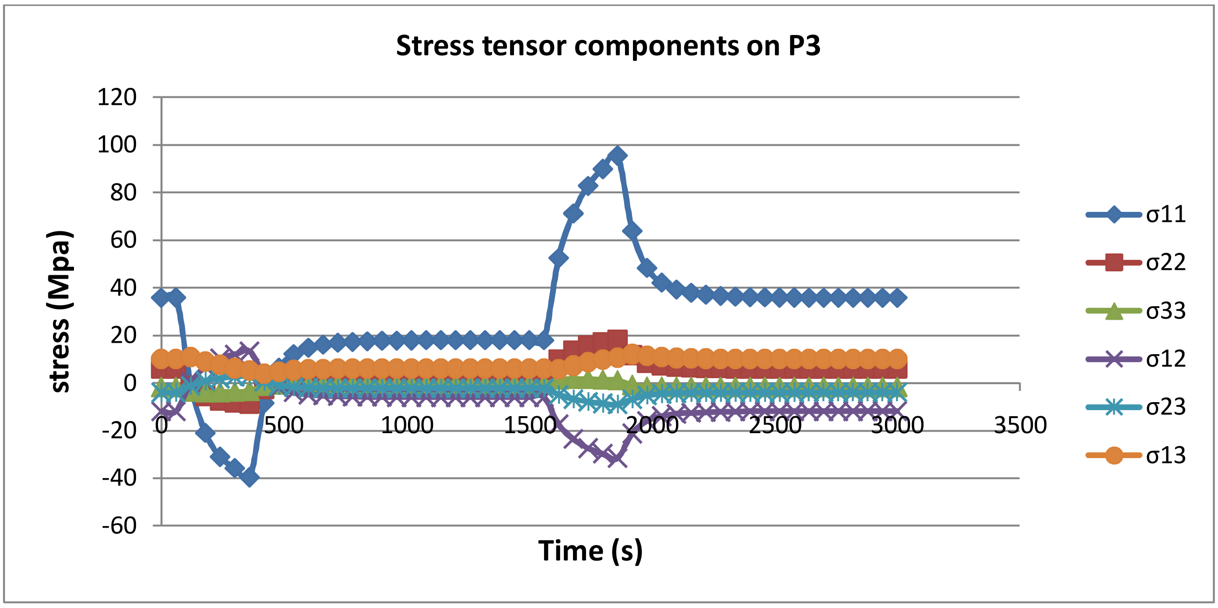

Figure 24 – Stress tensor on point P3 (800H)

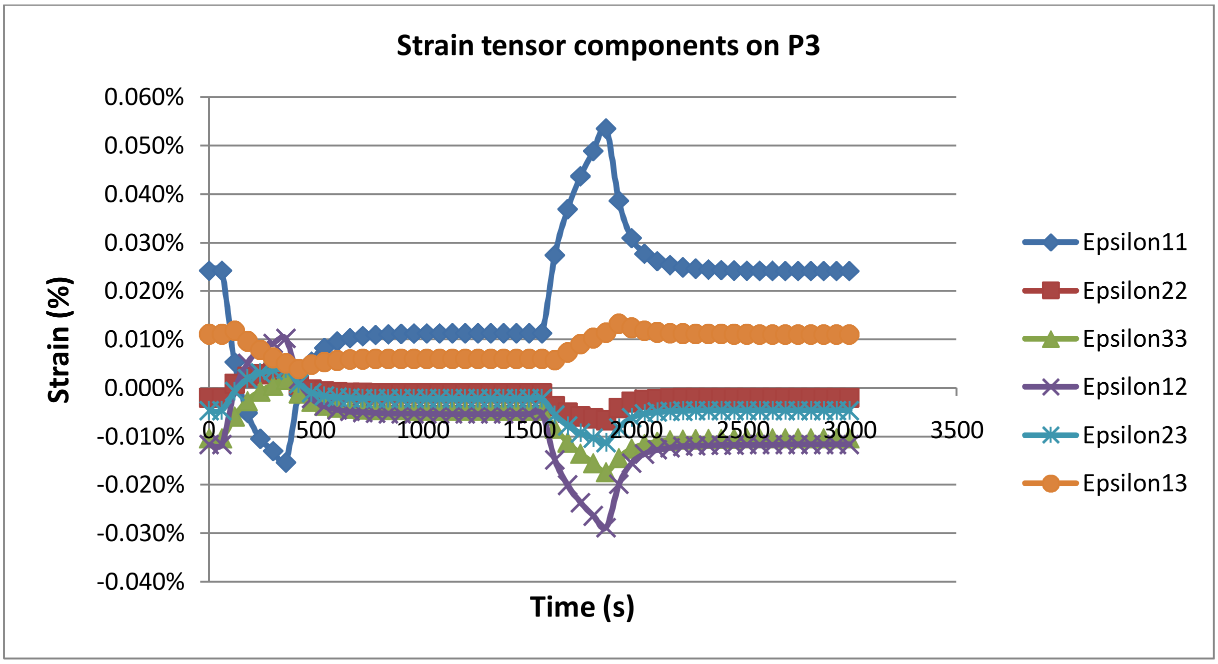

Figure 25 – Strain tensor on point P3 (800H)

Following the same procedure of fatigue analysis of ASME VIII div.2 we find:

$$\Delta\varepsilon_{eff} = \frac{102.76}{152136} + 33^{-5} = 0.101\%$$

The fatigue curve of Incoloy 800H gives a maximal allowable total strain of 0.2% for 10 000 cycles at 750℃. So we have a factor of 1.98 (0.2%/ 0.101%) as a safety margin in fatigue. Consequently, we have a safety margin less comfortable comparing with Inconel 617 material.

8. Summary of results

- Steady state Calculation

stress n°	side	position	Temperature	Stress	Life time			Temperature	Stress	Life time	
			°C	MPa	h	year		°C	MPa	h	year
1	hot	external plate	707.9	49.2	164 357	18.8		710.5	51.9	126 076	14.4
1'		external plate	706.6	55.4	109 858	12.5					
2	hot	collector middle	719.6	26.9	648 000	74.0		721.5	27.2	611 444	69.8
3	hot	collector basis	719.6	39.4	247 969	28.3		721.4	48.6	116 142	13.3
4	hot	collector basis	724.6	26.3	620 478	70.8		719.6	32.3	428 167	48.9
								744.7	23.5	537 840	61.4
6	cold	external plate	294.3	103.9	$>10^6$	$>10^6$		277.3	108.5	$>10^6$	$>10^6$
7	cold	collector basis	291.5	88.2	$>10^6$	$>10^6$		285.8	63.2	$>10^6$	$>10^6$
8	cold	corner	278.8	65.7	$>10^6$	$>10^6$		272.3	66.7	$>10^6$	$>10^6$

In the steady state calculation, we had seen that the application of a temperature gradient on the external plate and the taking into account of its thermal inertia has caused a degradation in terms of lifetime of about one year (from 13.3 to 12.5 year) and also, the appearance of a new critical zones particularly on the outer skin of the external plate.

- Transient Calculation

	Inconel 617 (only for information)	Incoloy 800H
Safety Margin rupture	5	/
Safety Margin fatigue (1000 cycles in 20 years)	8.7	1.98

Figure 26 –Comparative table

In transient calculation, we have estimated the margin of safety in fatigue as factor of 5 for the material Inconel 617 and we will make a study of the safety margin for the material Incoloy 800H as soon as we dispose the material characteristics in creep necessary for the calculation (April 2013).

9. Appendices

Description of model

Figure 1: Mesh of ¼ exchanger
Figure 2: material characteristics
Figure 3: boundary conditions

Steady state calculation with 617 material

Figure 4: Thermal load
Figure 5: Temperature field
Figure 6: Von Mises Stress
Figure 7: Comparative table of lifetime in creep
Figure 8 : Creep curve - lifetime: 109 858h

Transient calculation with 617 material

Figure 9: Piloting of temperature at primary inlet
Figure 10: Temperature hot side
Figure 11: Evolution of Von Mises Stress
Figure 12: Comparison of Von Mises Stress
Figure 13: Tensile strength of Inconel 617
Figure 14 –Strain tensor on point P1' (617)
Figure 15 –Stress tensor on point P1' (617)
Figure 16 –Stress tensor on point P3 (617)
Figure 17 –Strain tensor on point P3 (617)
Figure 18: Fatigue curve at 10 000 cycles of Inconel 617
Figure 19: Temperature in cold side
Figure 20: Von Mises stress in cold side

Transient calculation with 800H material

Figure 21 :Evolution of Von Mises stress (800H)
Figure 22 :Comparison of Von Mises stress (800H-617)
Figure 23 :Fatigue curve of Incoloy 800H (Alstom & Areva report)
Figure 24 – Stress tensor on point P3 (800H)
Figure 25 – Strain tensor on point P3 (800H)

Summary of results

Figure 26: Comparative table